M. Wójcik, J. Tejchman, and G. G. Enstad

Confined granular flow in silos with inserts — Full-scale experiments.

Confined granular flow in silos with inserts – full-scale experiments

M. Wójcik[1], J. Tejchman[1] and G. G. Enstad[2]
[1]Gdańsk University of Technology, Poland
mwojcik@pg.gda.pl, tejchmk@pg.gda.pl
[2]Tel-Tek Postec Dept., Porsgrunn, Norway
gisle.enstad@hit.no

Abstract

The paper describes results of experimental investigations of confined granular flow in a silo with different inserts. Over 100 experiments were carried out with dry cohesionless sand in a large metal silo with and without inserts at Tel-Tek, dept. POSTEC, in Norway. Wall pressures and flow patterns were measured during both silo filling and emptying. Three different insert types were used in the silo: double cone, cone-in-cone and inverted cone. Different positions of inserts were also investigated. Experimental results with inserts were compared with those without inserts. Some design recommendations for silos equipped with inserts were worked out.

Key words: silo flow, insert, filling, emptying, sand, experiments

1. Introduction

Silos are engineering structures widely used in industry to store, feed and process bulk solids. The flow pattern occurring in a silo is fundamental for the stresses acting on the silo walls. In silos, two main flow profiles can be distinguished, namely mass and funnel flow. During mass flow, the entire material is in motion and moves down with a velocity of the same order - the flow pattern is of a first-in and first-out type. This is usually achieved in silos equipped with steep smooth hoppers and large outlet diameters. Mass flow silos are frequently used in industrial processing because of some beneficial properties as: it is the most productive flow, problems like channeling, hang-ups, flooding of powders do not occur, stagnant regions are eliminated, and caking, degrading and segregation are minimized. The main disadvantage is that a steep hopper angle is required which makes the silo relatively tall. Moreover, the flowing material causes high dynamic wall stresses (in

particular at the bin/hopper transition) which requires thick silo walls. On the other hand, funnel flow is characterized by a first-in last-out sequence and assumes stagnant zones that reduce the silo capacity. It is suitable for hard abrasive free-flowing materials due to little wall wear. In stagnant regions, the bulk solid has a tendency to deteriorate or cake. Additionally, piping can occur when non-flowing materials are consolidated and the material still remains stable at the wall after the flow channel has been emptied. Wall stresses during discharge are slightly higher than during filling. Between mass flow and funnel flow, transition flow takes place which is characterized by a distinct flow change at a position depending on the filling height [1]. First, the entire material is in mass flow until it drops in the bin to a certain critical level below which funnel flow takes place. To predict the flow pattern in bulk solids, charts by Jenike [2] can be used, wherein the wall hopper inclination angle and hopper wall friction angle are the two most influential parameters (the flow pattern also depends slightly on the effective angle of internal friction).

To reduce significantly the size of stagnant zones and to change funnel flow into a more advantageous mass flow in existing silos, steeper and smoother hoppers may be used. However, this is often impossible due to the lack of space available or because of high retrofitting costs. An alternative to increasing the funnel flow diameter up to the silo diameter (and to achieve mass flow) are inserts, i.e. devices of a different shape placed inside the silo fill in a bin/hopper region to promote mass flow. Inserts, such as a double cone, a cone-in-cone, an inverted cone and others have been used for more than 40 years in the silo practice but very often with a limited success since consistent design rules for silo flow with inserts have not been developed yet and realistic criteria with respect to the type, size and location of inserts to be fulfilled to obtain mass flow are still lacking. An improperly designed insert may even lead to a more pronounced undesired funnel flow. Moreover, it is simply impossible to transfer existing design rules from silos without inserts to silos with inserts due to a different flow pattern.

The aim of our paper is to describe experimental results of flow patterns and wall pressures during filling and emptying of silos with inserts and to give some initial recommendations to the insert design (shape, size and location) with respect to mass flow of free-flowing cohesionless granular bulk solids [3]. The numerical FE simulations of the experiments [3] will be presented in the next paper. Our experiments in a full-scale metal silo were carried out at the Institute Tel-Tek in Norway. Over 100 tests in a large silo with inserts using dry and cohesionless sands were performed. Some experimental results have been already published with respect to the double cone [4] and cone-in-cone [5]. The innovative points of this paper are: a) the experimental results for an inverted cone (as compared to [4] and [5]), a double cone in a non-symmetric position (as compared

to [4]) and additional 5 configurations of a cone-in-cone (as compared to [5]), b) a comparison of the experimental data for all insert configurations and c) some recommendations for the insert design in large silos. In addition, the results in a silo without inserts were compared with the silo Eurocode.

2. Literature overview on experiments

Confined granular flow in silos containing different inserts has been experimentally investigated among others by Johanson and Kleysteuber [6], Johanson [7], [8], Nothdurf [9], Tuzün and Nedderman [10], Scholz [11], Strusch [12], Strusch and Schwedes [13], Enstad [14]-[16], Kobielak and Zamorski [17], Yang and Hsiau [18], Antonowicz [19], Johanson [20], Molenda et al. [21], Hsiau et al. [22] and Härtl [23].

Application of inserts in order to improve material flow patterns during emptying was originally proposed by Johanson and Kleysteuber [6], who showed that an inverted cone located at a specific position above the silo outlet significantly reduced the size of stagnant zones during funnel flow. They indicated a significant increase of wall stresses at the onset of discharge with an insert located in the upper part of the hopper, whereas the wall pressure peak did not appear with a small insert placed relatively close to the silo outlet. A large insert located in the upper part of a hopper was more effective to promote mass flow. Later, Johanson [7], [8] proposed a method to design a conical insert (so-called “Binsert”). Tuzün and Nedderman [10] investigated wall pressures and flow patterns in model silos with wedge-shaped and square inserts placed at various heights. During discharge, stagnant zones decreased. The obstacles inserted into the material increased the wall stresses during filling but decreased those during discharge. The inserts placed in the lower part of a silo had a more significant influence on the flow pattern compared to those located in the upper part of a silo. In turn, Strusch [12] performed tests in a model bin equipped with a hopper with various inclination angles and a triangular wedge placed symmetrically and non-symmetrically at different heights within a silo. During discharge, an increase of the normal wall stress was observed at the height of the upper edge of an insert. Below the insert, the normal wall pressure decreased since the insert carried a part of the material weight. An asymmetrically installed insert led to an asymmetric flow pattern and consequently contributed to a strong non-symmetric pressure distribution along the wall and insert. In laboratory experiments by Kobielak and Zamorski [17], the wall normal stress above a flat circular insert was the same as in the silo without inserts. Below the insert, the wall stress was significantly lower during filling and emptying. In a region above the insert, the wall

stress significantly increased during emptying. At the end of emptying, there was a sudden jump in the stress during a change of mass flow into funnel flow. The most comprehensive experimental investigations with silo inserts at laboratory scale were performed by Enstad [14]-[16], who used different inserts (cone-in-cone, double cone and inverted cone). From his experiments with a cone-in-cone, some important suggestions were obtained. The inclination of the internal cone to the vertical α had to be smaller than the critical wall inclination for mass flow α_c (Fig.1). In turn, the inclination of silo hopper walls to the vertical could be twice as large as the critical inclination angle for mass flow. In small model silos with free flowing materials (such as anthracite and PVC powders) to obtain mass flow, the top of the cone-in-cone had to be above the transition point between cylinder and hopper and its height should be similar as the hopper height. The inlet ratio I (ratio between the material area inside and outside of the internal cone at its top) and the outlet ratio O (ratio between the material area inside and outside of the internal cone at its bottom) should be for free-flowing powders about I=0.7 and O=0.15 (plane flow silo) and I=1.0 and O=0.1 (axisymmetric silo), respectively. In the case of a double cone, an insert position was crucial to obtain symmetric mass flow with the optimum insert diameter equal to 25% of the silo diameter. For an inverted cone, its smaller inclination to the vertical (e.g. 17.5^o) was more effective than its larger inclination (e.g. 25^o or 40^o) to achieve mass flow. The position of its top should be above the bin/hopper transition.

Summarized, there still exist too little experimental investigations on solid flow in silos with inserts. The experiments were mainly performed with model silos. Thus, a direct transfer of these results to full-scale silos is not possible due to size effects caused by a different stress level (influencing mobilized internal friction angle, mobilized dilatancy angle and cohesion of the solid), a different ratio between the silo size and mean grain size of the solid and stochastic distribution of solid parameters [24], [25]. Since our tests were conducted with dry sand only, the obtained results are valid for cohesionless bulk solids similar to sand (e.g. cohesion can affect the results as cohesive arching has to be taken into account).

3. Experimental set-up

The tests were conducted in a cylindrical metal silo 9 m high with an inner diameter of 2.5 m (Fig.2). The geometry of the symmetric conical hopper was: 1.25 m (height), 44^o (inclination angle to the vertical) and 0.1 m (outlet diameter). The total volume of the material was 26 m^3. The inlet and outlet of the silo were centrally located. During emptying, the material was discharged freely by

gravity. Concentric filling was performed with a filling rate of about 10-15 m^3/h. The emptying rate was 17-25 m^3/h. Dry and cohesionless initially loose sand used in the experiments had the following properties: volumetric weight of γ=13.7 kN/m^3, angle of repose of ϕ=36° and wall friction angle of φ_w=22° (sand '1' in the silo with a double cone [4]), and γ=14.5 kN/m^3, ϕ=35° and φ_w=17° (sand '2' in the silo without inserts and silo with other inserts [5]). The critical hopper wall angle for mass flow to the vertical was equal to 20° (sand '1') and 29° (sand '2') with the safety margin of 4^o [4], [5], as recommended by Jenike [2] to be on the safe side when designing silos for mass flow (the critical hopper wall angle from the diagram by Jenike [2] was decreased by 4^o).

To investigate approximately the flow pattern, small markers with a diameter of 30 mm were placed at fixed positions in the silo during filling (7 levels with 9 markers and 2 levels with 5 markers) using steel tubes in two orthogonal planes along the silo diameter (Fig.3). During filling, when the lower end of the tube was covered with sand, the markers were dropped through the pipe. The tube was then gradually pulled up to the next level, all the time making sure that the lower end of the pipe was inside the stagnant sand. This procedure was repeated until the silo was completely filled. During discharge, numbered markers passing through the outlet were detected and the residence time for each marker was noted.

The wall stresses were measured with the aid of 10 pressure cells mounted along the wall, 7 in the hopper (H1-H3, T4-T7) and 3 in the cylindrical part (C8-C10) (Fig.4). The cells T4-T7 were placed at the same level just below the bin/hopper transition to investigate the wall pressure distribution along the silo circumference. Each cell measured both normal and tangential loads in the hopper (based on a strain gauge technology), except of cells C8-C10 located along the bin wall which measured only the normal stress. The pressure cells with a diameter of 120 mm interacted with the material surface and were made using the material cut from the silo wall. Thus, the surface of each cell had the same both roughness and curvature as the silo wall. During installation, great care was undertaken to ensure alignment with the inner face of the silo wall. The small round gap between the cell and silo wall was filled with elastic silicon paste. The pressure signals were recorded with a frequency of 500 Hz. Before the pressure cells were used, a calibration was performed. Each pressure cell mounted in the silo was calibrated in the normal and tangential directions. For each pressure cell, several different weights were chosen within the experimental pressure range. The calibration process showed a linear response of the pressure cells subjected to different loads. The load cell stiffness in the normal direction was 600 N/mm.

Experiments were carried out in the silo without inserts and with inserts (Fig.5). Various insert types and their positions were investigated (Fig.6) to find both the most efficient type and location to promote mass flow in a silo. In the case of double cones, a 1.62 m steel insert was used with a diameter of about 1/4 of the hopper diameter as recommended by Enstad [16] (Fig.5a). The insert had a taller upper cone of 15^o to the vertical pointed upwards and a shorter lower cone of 30^o pointed downwards. The inclination angle of the upper cone to the vertical, 15°, was chosen based on small-scale tests by Enstad [16]). The difference between the hopper wall inclination of 44° and the inclination of the lower cone of 30° to the vertical was 15^o less than the critical inclination angle for mass flow in hoppers of 29° [2]. In addition, the inverse configuration of a double cone was also tested. One assumed 6 different configurations for double cones (5 symmetric locations DC I–DC V and 1 non-symmetric one against the vertical axis DC IVa). Four double cones were in their normal position (DC III, DC IV, DC IVa and DC V) and two double cones were inverted (DC I and DC II), i.e. the smaller cone part was at the top. In the case of the cone-in-cones CC I and CC II (Fig.5b), mass flow was expected since the insert inclination of 21^o and the difference between the insert inclination and the inclination of the hopper walls of 23^o were below the critical wall angle for mass flow of 29^o. Two different cone-in-cone types were tested (Fig.6): 3 with a single internal hopper (CC I - CC III) and 3 with a double internal hopper (CC IV-CC VI). For the cone-in-cones CC I and CC II, the inlet I and outlet O ratios were 0.15 and 0.03, respectively, whereas for the cone-in-cones CC III - CC VI, they were equal to I=0.37 and O=0.1, respectively. The diameter of the larger internal hopper at the top was 0.86 m (CC I and CC II) or 1.3 m (CC III - CC VI), and at the bottom was 0.1 m (CC I - CC VI). Its wall inclination to the vertical was 21° (CC I and CC II) or 31° (CC III-CC VI). In the case of the smaller internal hopper, the diameter at the top was 0.48 m, the diameter at the bottom again 0.1 m and the wall inclination to the vertical 15°. The minimum distance between the silo hopper and the larger internal cone was equal to the outlet diameter (CC VI), to two outlet diameters (CC I, CCC IV, CC V) and to four outlet diameters (CC II). The minimum distance between the two internal cones was equal to two outlet diameters (CC V) or to one outlet diameter (CC IV and CC VI). Additionally an inverted cone was used (the largest internal cone of Fig.5b was simply placed upside-down in the hopper with its top closed) (Fig.5c). The maximum diameter of the inverted cone IC I was equal to 50% of the silo diameter and its inclination to the vertical was 31^o similar to the wall inclination angle for mass flow, 29^o [2] (Fig.6).

The experimental results with inserts were compared with the corresponding ones carried out in the silo without inserts (denoted as “0”, Fig.6).

4. Experimental results

4.1 Silo without inserts

Figure 7a shows the surface profiles of sand observed from the silo top for two different cross-sections of Fig.3 (sections '5-1-0-3-7' and '8-4-0-2-6') and Fig.7b shows the emptying times for markers located at different silo levels in the section 5-1-0-3-7 of Fig.3. At the end of filling the surface profile had a shape of a conical heap with an inclination angle of 33^{o}. When the outlet was opened, the material started to flow just in the silo centre by changing the initial conical surface profile into the shape of a dip. The silo fill exhibited funnel flow during the entire discharge. First, the markers at the central axis were rapidly discharged. Then, the markers located away from the internal flow channel moved. They were discharged in a reverse order, i.e. the markers located at higher levels came out before those at lower levels. The central rapidly flowing channel was surrounded by a slowly flowing zone [4], whereas the material located adjacent to the wall remained stagnant until it was exposed at the top. The markers located close to the silo wall in the hopper and near the silo transition came out last. Although the silo filling was symmetric, the flow profile was slightly non-symmetric (Figs.7a and 7b). The diameter of the flowing channel was maximum 1.2 m based on the movements of the markers in the sand (Fig.7b).

Figure 8 presents a normal wall stress evolution during silo filling and emptying for one of the tests. The distribution of mean wall normal and shear stresses measured in several tests during filling and emptying is presented in Fig.9. During filling, each curve in the bin followed a similar distribution trend as given by the Janssen theory (i.e. the stress gradient diminished during continuous filling and each curve approached its asymptote), Figs.8 and 9a. As the silo was discharged, the normal wall stress immediately slightly increased, stayed nearly constant for a period, and then decreased, Fig.8. The results were found to be repeatable (the maximum coefficient of the stress variation was 15%). The largest filling normal wall stress appeared at the transition between bin and hopper (it was equal to 13 kPa in the lower part of the bin at the cell C8 of Fig.4) and 22.3 kPa in the upper part of the hopper at the cell H3 of Fig.4). At the onset of granular flow, a slight increase of normal wall stresses was mainly observed. This increase was caused by solid dilatancy in the flow region. It was rather small due to the occurrence of funnel flow. The increase was about 15-21% (lower and mid-part of the bin at the cells C8 and C9 of Fig.4) and 11% (upper part of the hopper at the cell H3 of Fig.4), respectively. In the lower hopper wall, the normal pressure decreased by 13% (cell H1 of Fig.4). The maximum normal stress during flow was equal to 15 kPa in the lower part of the bin and

24 kPa in the upper part of the hopper. In turn, the wall shear stress increased along the hopper wall during emptying by 30-50% (from 5.5 kPa up to 8.5 kPa and from 7.8 kPa up to 10.5 kPa).

Comparing to Eurocode 1 [26], the maximum measured normal stresses were smaller by 24% (bin) and by 44% (hopper) during filling and by 23% (bin) and by 41% (hopper) during discharge for symmetric loads (Fig.9a). The standard values using the so-called base method for hoppers were calculated with the parameters for sand '2' used in silo tests: γ=14.5 kN/m^3, ϕ=35° and φ_w=17°. These comparative results indicate that the standard values may strongly over-predict wall pressures (in particular in hoppers) if the solid is initially loose and uniformly distributed during filling. Due to its simplicity (solid deformation is not included), the standard formulas are not always able to capture realistically the solid behaviour. In turn, the pressure difference between filling and emptying and the maximum wall shear stresses in the hopper were similar in experiments. Note, that for shallow hoppers the standard wall stresses are the same for filling and emptying [26]. The increase of the experimental normal stresses at the transition (difference between the stresses in the lower part of the bin and upper part of the hopper) was about two times smaller than given by Eurocode [26] (Fig.9a). A significant wall pressure variation along the silo circumference at the transition at the end of filling and at the beginning of emptying was obtained (Fig.9b). The maximum differences between the highest (32 kPa) and the lowest normal stresses (22 kPa) along the transition circumference at the beginning of emptying were even 37 %. Such a large stress variation along the silo circumference is not taken into account by Eurocode 1 [26] which causes a stress increase solely by 12% (during filling) and by 24% (during emptying) in the horizontal wall normal stress in our experimental silo (based on calculations of the additional wall pressure representing non-symmetric horizontal loads and imperfections in bulk solids).

4.2 Silo with double cone

Figure 10 shows surface profiles and times for markers in the silo containing a double cone in its up-side-down position (DC I). With double cones installed, the flow channel considerably widened (compare Figs.7b and 10b) but mass flow was not achieved in any of its 6 different positions. All experimental results were very similar independently of the insert configuration in its symmetric position against the vertical axis with resembling flow patterns. At the beginning of discharge, the upper part of the sand moved slowly down both in the silo centre and along the wall. When the discharging process proceeded, the diameter of the fast flowing channel observed from the top became smaller and smaller, until the surface profile reached a dip shape and sand started to slide down on the surface. Thus, the markers in the mid-region (at the distance of 1.2 m) came out first in

a mass flow order, but markers located adjacent to the walls came out down in a reverse sequence, level by level implying that sand close to the wall remained stagnant until the markers were caught up with the surface flow. The inclination angle of the upper part of the cone to the vertical 15°(smaller by 5^o than the critical angle for mass flow) caused a uniform distribution of the material velocity in the region above the insert. The average diameter of the flowing channel was between 1.2 m and 2.3 m (based on the results of Fig.10b).

The most uniform axisymmetric silo discharge was obtained with a symmetric insert located at the lowest level (DC I). The other 4 different symmetric insert positions caused flow to be non-uniform. A completely skew flow was achieved with a tilted insert DC IVa (the bottom apex was displaced by 5 cm from the central vertical line) (Fig.11).

During silo emptying with double cones, wall stresses showed a slightly oscillating character (see the wall stress evolution at the pressure cell H3 in Fig.12). Figures 13a and 13b present the mean wall stress distribution obtained from several tests with the double cone DC I. At the end of filling and at the beginning of emptying, the coefficient of variation was up to 13%. The maximum normal stresses measured during filling were near the silo transition (11 kPa in the bin and 29 kPa in the hopper). It has to be noted that these values were registered at the cell C9 only (3.05 m above the silo outlet) due to technical problems at the cell C8 (2.17 m above the silo outlet). At the onset of discharge, the wall stresses increased in the hopper slightly below the transition (the normal wall stress up to 25% and shear wall stress up to 76%) and in the bin above the transition (the normal wall stress by 35%). In the lower part of the hopper, the normal wall stress decreased by 25% and the shear stress remained unchanged. The maximum stresses during emptying were again at the silo transition (the normal wall stress was 14.2 kPa in the bin and 30.7 kPa in the hopper, and the shear stress was 14.6 kPa in the hopper).

As compared with tests without inserts, the double cone caused a stronger increase of stresses during discharge in the upper hopper part and in the lower bin part. This increase was in the hopper larger by 28% (wall normal stress) and by 41% (wall shear stress), and in the bin by 25% (wall normal stress). In turn, the wall normal stress in the lower hopper part was lower by 56%. The differences between the highest and lowest wall stresses around the silo perimeter at the transition were 16%.

Figures 14a and 14b present the stress results for the silo with the non-symmetric insert (DC IVa). The stress results along the wall height were similar to those with the insert DC I. At the end of

filling and at the beginning of emptying, the coefficient of variation was 10%. After filling, the maximum normal stresses were 9 kPa in the bin and 25 kPa in the hopper. At the beginning of discharge, the wall normal stresses increased in the bin up to 45% (13.4 kPa) and hopper up to 25% (31 kPa), except of the lower hopper part, where the wall normal stress decreased by 26%. Due to an eccentric position of the insert, sand moved at one side. At the onset of discharge, the wall normal stress close to the flowing channel decreased (by 5%) whereas in other places at the transition, the stress increased (up to 25%). The shear stress increased along the entire circumference by 70% (Fig.14b).

Summarized, the double cone diameter was significantly too small to change funnel flow into mass flow (the type of the insert and cone inclinations were of minor importance). The insert should be placed in a symmetric position against the central axis at the lowest possible position.

4.3 Silo with cone-in-cone

Figure 15-17 shows the surface profiles and times for markers during emptying in the silo with 3 different cone-in-cones (CC I, CC III and CC IV). Similarly as for the double cone, the cone-in-cones caused the flow channel to be wider than in the silo without inserts. Moreover, the slowly flowing zone that was located around the rapidly flowing channel was also wider as compared with the silo without inserts, approaching the silo diameter. At the beginning of emptying, the entire upper sand surface was in motion. However, sand close to the silo wall had a smaller velocity than the sand located in the silo centre. Later, the surface profile reached the shape of a dip and sand started to slide down along its surface. The narrowest flow channel was observed with the single cone-in-cone CC III (with the wall inclination to the vertical of α=31^{o} - higher by 2^{o} than the critical mass flow angle [2]). The rapid flow channel was surrounded by a wide slowly-flowing zone - flow was more similar as in a silo without inserts. The markers at mid-radius positions came out in a fairly erratic manner probably due to the fact that they were located just on the flow border. In turn, the flow channel in the silo with the cone-in cone CC I (wall inclination to the vertical of α=21^{o} - smaller by 8° than the critical angle for mass flow [2]) was similar as in tests using double cones. The markers at the centre and between the centre and silo wall were discharged almost in a mass flow order, and the markers located close to the wall came out in a reverse order as during funnel flow. The most effective configuration to promote mass flow was the double cone-in-cone CC IV (the wall inclination to the vertical of the large internal cone was α=31^{o} and of the small internal cone α=15^{o}). The flow channel with CC IV was wider than previous ones. This could be

noticed based on the top surface profile that remained unchanged during almost 1/3 of the total emptying time (Fig.17a) and also based on the resident time of markers (Fig.17b), where the difference in the emptying time between the markers located at the same level in the upper half of the silo (levels VI, VII, VIII) was significantly smaller that in the previous cases (e.g. for CC I). The results indicate that for a single internal cone-in-cone, the insert diameter should be significantly larger. The higher position of the insert CC IV was more effective than in its lowest position (CC VI) with respect to mass flow. In this case, the minimum distance between the silo hopper and larger internal hopper (CC VI) was equal to the outlet diameter and for CC IV this distance was twice as large as the outlet diameter. In turn, the distance between the two internal cones was more beneficial for CC IV (equal to one silo outlet diameter) than for CC V (equal to two outlet diameters).

The mean wall stresses at the end of filling and at the beginning of emptying from all pressure cells along the silo height and around the circumference at the transition are shown in Figs.18-20 for CC I (Fig.18), CC III (Fig.19) and CC IV (Fig.20). The results were found to be repeatable. The maximum pressure coefficient of variation at the end of filling and beginning of emptying was 14% (CC I), 20% (CC III) and 13% (CC IV), respectively. At the end of filling, the maximum wall normal and shear stresses for the three insert configurations were obtained in the upper part of the hopper. The highest wall normal stress was measured with the double cone-in-cone (CC IV): 13 kPa in the bin and 35 kPa in the hopper. For all insert configurations, the stress distribution around the transition was strongly non-uniform (the differences were about 20-70%). During emptying, the wall stresses increased in the bin at the transition and in the upper part of the hopper, and decreased in the lower part of the hopper. In the lower part of the bin, the normal wall stress increased up to 28% (CC I), 16% (CC III) and 82% (CC IV), respectively, which reflected the flow profile in the silo (the wider the flow channel, the higher are the wall normal stresses). In the case of CC I, the wall normal stress in the hopper at the transition increased up to 26%, whereas the shear wall stress increased by 135%. For the insert CC III, the normal wall stress in the hopper right below the transition increased up to 46% (except of the cell T4 where the stress decreased by 30%) and the wall shear stress up to 24%. When the insert CC IV was used, the wall normal stress increased up to 45% and the shear wall stress up to 159%. The almost entire height of the hopper (except of the transition region) was significantly unloaded since most of the material weight was carried by the insert. This significant reduction of the wall normal stress in the lower part of the hopper was 33% (CC I), 58% (CC III) and 56% (CC IV), respectively. The maximum stresses during emptying were at the silo transition: the normal wall stress was 24 kPa in the bin and 30 kPa in the hopper, and the shear stress was 18 kPa in the hopper (for CC IV).

4.3 Silo with inverted cone

An inverted cone IC I converted funnel flow into almost mass flow (Fig.21). When discharge started, the sand surface profile formed after silo filling started to move uniformly downwards and its conical shape remained the same for a long time. The flow profile was similar to mass flow except of the last emptying stage where it changed into funnel flow. Almost all markers came out in a mass flow order, i.e. lines in Fig.21b were almost horizontal and markers located at the lowest level came out first. Only some markers located close to the wall at the transition came out as the last ones due to a small stagnant zone at the transition. Sand above the insert had a smaller flow velocity than sand between the centre and silo wall since the wall inclination of the cone to the vertical, 31^{o}, was higher than the critical mass flow angle for hoppers (by 2^{o}).

The maximum normal and shear wall stresses after filling were in the upper part of the hopper: 26 kPa (normal stress) and 11 kPa (shear stress) (Fig.22). Small wall stresses in the hopper during filling and emptying were caused by the fact that most of the material weight was taken by the insert. During emptying, wall pressures pulsated strongly (Fig.23). The maximum wall normal stress was 18 kPa (bin) and 27 kPa (hopper). The maximum wall normal stress increase in the bin was obtained during emptying above the transition (about 36%). In the hopper below the transition, the maximum growth of the wall normal stress was by 45% (except the pressure cell T5, where the pressure decreased by about 10%). The shear wall stress increased below the transition up to 195%. In the hopper (except of the transition region), the wall normal and shear stresses decreased; the wall normal stress decreased up to 78% and the shear wall stress decreased up to 75%. The maximum stress coefficient of variation at the end of filling and beginning of emptying was 22%. Summarized, the insert diameter (50% of the silo diameter) was sufficient to promote mass flow. The wall inclination to the vertical should be smaller than 31°.

Figures 24 and 25 summarize our experimental results of wall stresses during the end of filling and beginning of emptying. During filling of the silo with inserts, the wall normal stresses did not change in the bin, and they increased in the hopper below the transition and decreased in the lower part of the hopper as compared to the cases without inserts (Fig.24a). In turn, during emptying of the silo with inserts, the wall normal stresses increased in the bin, they increased in the hopper below the transition and they decreased in the lower part of the hopper (Fig.24b). The highest wall normal stress in the bin during discharge was for the double cone-in-cone CC IV (24 kPa) and at the transition in the hopper for the double cone DC I (31 kPa). The maximum wall normal stresses were

significantly smaller in the entire silo during filling as compared to Eurocode 1 [26]. For emptying they were smaller by about 30% in the hopper and larger by 20% in the bin (CC IV). The wall stresses around the transition were more uniform during filling (Fig.25a) than during flow (Fig.25b).

5. Conclusions

The main outcomes from our experiments in a full-scale silo containing cohesionless sand are the following:

Due to size effects caused mainly by the pressure level, experimental results of stresses cannot be directly transferred from model silos to large ones. Recommendations with respect to the size and location of silo inserts obtained on the basis of small scale tests turned out wrong in tests in a large silo.

In the silo without inserts, funnel flow was obtained with a narrow flow channel in the silo centre and wide dead zones along the silo walls. The flow channel was considerably wider in the silo with inserts and its diameter strongly depended on the insert type. However, ideal mass flow was never obtained in any of the insert configurations. The inverted cone (IC I) was the most efficient insert to promote mass flow mostly due to its large size. It changed funnel flow into almost mass flow with a very narrow stagnant zone located close to the silo transition. Silo flow was always non-symmetric and the flow eccentricity was higher when inserts were installed.

The stress distribution in the silo with inserts was dependent upon the width of the flow channel and the position and shape of the insert which determined the magnitude of volume changes. During filling, the distribution of wall stresses in the bin was not dependent upon the insert presence, whereas in the hopper it was dependent. The normal and shear wall stresses were higher with inserts by 15-50% in the upper part of the hopper close to the transition. The largest stresses occurred with the double cone-in-cone CC IV. Significant stress variations of 20-40% along the circumference at the transition occurred during filling, which were similarly independent of the presence of inserts or its shape and location (e.g. for the silo without inserts 37% and for the silo with large cone-in-cone 41%).

The wall stress evolution during silo discharge with inserts was more chaotic and more oscillating compared to the stress evolution in the silo without inserts. The stress changes were also more

significant in the silo with inserts than in the silo without inserts due to the widening of the flow channel. At the beginning of emptying in the silo without inserts, the maximum normal wall stress occurred below the bin/hopper transition. In the case of the silo with inserts, it occurred at a higher position, i.e., at the transition and above it. The wall normal stress increased with inserts almost in the entire silo by 20-60% (the lower part of the bin) and by 45% (the upper part of the hopper at the transition), except of the lower part of the hopper (close to the insert and below it), where it strongly decreased even up to 90% since the insert carried a part of the solid weight. The largest wall normal stress changes as compared with the silo without insert, occurred with the double cone-in-cone CC IV (bin), with the double cone DC I (the upper part of the hopper) and with the inverted cone IC I (the lower part of the hopper). Pronounced stress variations of max 40% for IC I and 70% for CC III along the circumference at the transition occurred during emptying. The variations were higher in the silo with inserts than in the silo without them.

Since the double cones turned out to be too small to change flow into mass flow in experimental silos, their maximum diameter should be significantly larger than 25% of the silo hopper diameter (e.g. 50% as in the case of the inverted cone which produced almost quasi-mass flow). All inserts should be placed in a symmetric position against the silo central axis.

A larger difference between the wall inclination to the vertical of the upper part of the double cone, inverted cone and cone-in-cone and the critical angle for mass flow in hoppers was more advantageous to obtain the uniform solid flow directly above the insert.

For the double cone-in-cone, the presence of the smaller internal cone decreased the width of stagnant zones. Its inclination to the vertical may be equal to the half of the larger internal cone. The minimum distance between the silo hopper and larger internal cone twice greater than the outlet diameter and the minimum distance between two internal cones equal to the outlet diameter were more effective to decrease stagnant zones close to the silo wall (than one outlet diameter and two outlet diameters, respectively).

Acknowledgement

The first author is grateful to the Norwegian Research Council, the industrial members of POSTEC, and the European Marie Curie programme for financial support, and the Telemark University College for preparation of the experimental equipment. The authors acknowledge the contributions to the experiments by Johannes Härtl and Songxiong Ding.

References

[1] Benink, E., 1989. Flow and stress analysis of cohesionless bulk materials in silos related to codes. *PhD Thesis*, University of Twente, Enschede.

[2] Jenike, A. W., 1964. Storage and Flow of Solids. *Bulletin No 123 of the Utah Engineering Experiment Station*, University of Utah, 53, 26.

[3] Wójcik, M., 2009. Experimental and theoretical investigations of flow pattern and wall pressures in silos with and without inserts. *PhD Thesis*, Gdańsk University of Technology.

[4] Wójcik, M., Härtl, J., Ooi, J. Y., Rotter, J. M., Ding, S. and Enstad, G. G., 2007. Experimental investigation of flow pattern and wall pressure distribution in a silo with double-cone insert. *Particle & Particle System Characterization* 24, 4-5, 296-303.

[5] Härtl, J., Ooi, J. Y., Rotter, J., M., Wójcik, M., Ding, S. and Enstad, G. G., 2008. The influence of a cone-in-cone insert on flow pattern and wall pressure in a full-scale silo. *Chemical Engineering Research and Design* 86, 370-378.

[6] Johanson, J. R. and Kleysteuber, W. K., 1996. Flow corrective inserts in bins. *Chemical Engineering Progress* 62, 11, 79-83.

[7] Johanson, J. R., 1967. The placement of inserts to correct flow in bins. *Powder Technology* 1, 328-333.

[8] Johanson, J. R., 1982. Controlling flow patterns in bins by use of inserts. *Bulk solid handling* 2, 3, 495-498.

[9] Nothdurft, H., 1976. Schuttgutlasten in Silozellen mit Querschnittsvergengungen. *PhD Thesis*, Techn. University of Braunschweig, Germany.

[10] Tuzün, U. and Neddermann, R. M., 1983. Flow of granular materials round obstacles. *Bulk Solids Handling* 3, 507-517.

[11] Scholz, V., 1988. Untersuchungen zur Anordnung starrer koaxial Einbauten in Schüttgutbehaltern. *PhD Thesis*, Wilhem-Pieck-Universitat Rostock.

[12] Strusch, J., 1996. Wandnormalspannungen in einem Silo mit Einbau und Kräfte auf Einbauten. *PhD Thesis,* Technische Universität Braunschweig, Germany.

[13] Strusch, J. and Schwedes, J., 1996. Silos with inserts - wall normal stresses and forces on inserts. *ZKG International* 49, 12.

[14] Enstad, G. G., 1996. Investigation of the use of insert in order to obtain Mass Flow in Silos. *POSTEC-Newsletter No. 15*, 13-16.

[15] Enstad, G. G., 1996. Further investigation of the use of insert in order to obtain mass flow in silos. *POSTEC-Newsleter* No. 16, 15-18.

[16] Enstad, G. G., 1998, Use of inverted cones and double cones as inserts for obtaining mass flow. *POSTEC-Newsleter* No. 17*,* 15-16.

[17] Kobielak, S. and Zamorski, A., 2000. Redistribution of grain pressure in silos with inserts. *The Third Israeli Conference for Conveing and Handling of Particular Solids,* Israel.

[18] Yang, S. C. and Hsiau, S. S. (2001). The Simulation and Experimental Study of Granular Materials Discharged From a Silo With the Placement of Inserts. Powder Technol., 120(3), 244–255,

[19] Antonowicz, R., 2004. Effect of geometric parameters of reducing devices on flow pattern and load distribution in silos with large diameters (in polish). *PhD Thesis*, Politechnia Wrocławska, Poland.

[20] Johanson, K., 2006. Predicting cone-in-cone blender efficiencies from key material properties. *Powder Technology* 170, 3, 109-124.

[21] Molenda, M., Montross, M. D. and Horabik J., 2007. Non-Axial Stress State in a Model Silo Generated by Eccentric Filling and Internal Inserts. *Particle&Particle Systems Characterization* 24, 291-295.

[22] Hsiau, S. S., Smid, J., Tsai, S. A., Tzeng, C. C. and Yu, Y. J., 2008. Flow of filter granules in moving granular beds with louvers and sublouvers. *Chemical Engineering and Processing* 47, 2084–2097.

[23] Härtl, J., 2008. A study of granular solids in silos with and without an insert. *PhD Thesis*. The University of Edinburgh.

[24] Tejchman, J. and Gudehus, G., 2000. Verspannung, Scherfugenbildung und Selbsterregung bei der Siloentleerung. "Silobauwerke und ihre spezifischen Beanspruchungen", *eds.: J. Eibl and G. Gudehus, Deutsche Forschungsgemeinschaft,* Wiley-VCH, 245-284.

[25] Tejchman, J., 2008. *FE modeling of shear localization in granular bodies with micro-polar hypoplasticity*. Springer Series in Geomechanics and Geoengineering (eds. W. Wu and R. J. Borja), 2008.

[26] EN1991-1-4. Eurocode 1: Basis of design and action on structures. Part 4: Actions in silos and tanks. Brussels: CEN, 2006.

LIST OF FIGURES

Fig.1: Sketch of cone-in-cone configuration (α_c – critical mass flow wall angle in hoppers, *I* and *O* - ratios between the horizontal material area inside and outside of internal cone at its top and bottom, respectively)

Fig.2: Silo used in experiments: a) geometry of silo, b) view of experimental silo with rectangular feeder metal silo

Fig.3: Positions of markers in sand

Fig.4: Pressure cells and their positions along silo walls

Fig.5: Inserts used in experiments a) double cone, b) cone-in-cone, c) inverted cone

Fig.6: Different insert configurations during experiments (test "0" is related to silo without inserts) (dimensions are in [m])

Fig.7: Experimental results for silo without insert: a) surface profiles of flowing sand and b) emptying times for markers located at different levels in cross-section 5-1-0-3-7 of Fig.3 (numbers indicate level distances from outlet in [m], Fig.3)

Fig.8: Evolution of normal wall stresses on silo wall without inserts (from one arbitrary test)

Fig.9: Mean normal and shear wall stresses obtained from several tests in silo without inserts: a) along silo height and b) around bin/hopper transition ('a' - according to standard [26])

Fig.10: Experimental results for silo with inverted double cone DC I: a) surface profiles of flowing sand and b) emptying times for markers located at different levels in cross-section 5-1-0-3-7 of Fig.3 (numbers indicate level distances from outlet in [m], Fig.3)

Fig.11: Experimental results for silo with double cone DC IVa in non-symmetric position: a) surface profiles of flowing sand and b) emptying times for markers located at different levels in cross-section 5-1-0-3-7 of Fig.3 (numbers indicate level distances from outlet in [m], Fig.3)

Fig.12: Evolution of wall normal stresses in silo with inverted double cone (DC I)

Fig.13: Distribution of mean wall normal and shear stresses obtained from several tests in silo with inverted double cone DC I: a) along silo height and b) around bin/hopper transition

Fig.14: Distribution of mean wall normal and shear stresses obtained from several tests in silo with double cone DC IVa (non-symmetric position, Fig.6): a) along silo height and b) around bin/hopper transition

Fig.15: Experimental results for silo with cone-in-cone CC I: a) surface profiles of flowing sand and b) emptying times for markers located at different levels in cross-section 5-1-0-3-7 of Fig.3 (numbers indicate level distances from outlet in [m], Fig.3)

Fig.16: Experimental results for silo with cone-in-cone CC III: a) surface profiles of flowing sand and b) emptying times for markers located at different levels in cross-section 5-1-0-3-7 of Fig.3 (numbers indicate level distances from outlet in [m], Fig.3)

Fig.17: Experimental results for silo with cone-in-cone CC IV: a) surface profiles of flowing sand and b) emptying times for markers located at different levels in cross-section 5-1-0-3-7 of Fig.3 (numbers indicate level distances from outlet in [m], Fig.3)

Fig.18: Distribution of mean wall normal and shear stresses obtained from several tests in silo with cone-in-cone CC I: a) along silo height and b) around bin/hopper transition

Fig.19: Distribution of mean wall normal and shear stresses obtained from several tests in silo with cone-in-cone CC III: a) along silo height and b) around bin/hopper transition

Fig.20: Distribution of mean wall normal and shear stresses obtained from several tests in silo with cone-in-cone CC IV: a) along silo height and b) around bin/hopper transition

Fig.21: Experimental results for silo with inverted cone IC I: a) surface profiles of flowing sand and b) emptying times for markers located at different levels in section 5-1-0-3-7 of Fig.3 (numbers indicate level distances from outlet in [m], Fig.3)

Fig.22: Distribution of mean wall normal and shear stresses obtained from several tests in silo with inverted cone IC I: a) along silo height and b) around bin/hopper transition

Fig.23: Evolution of wall normal stresses in silo with inverted cone IC I

Fig.24: Distribution of mean wall normal and shear stresses along silo height obtained from several tests in silo with different inserts during filling (a) and beginning of emptying (b) (‘a’ -according to silo standard [26])

Fig.25: Distribution of mean wall normal and shear stresses around bin/hopper transition obtained from several tests in silo with different inserts during filling (a) and beginning of emptying (b)

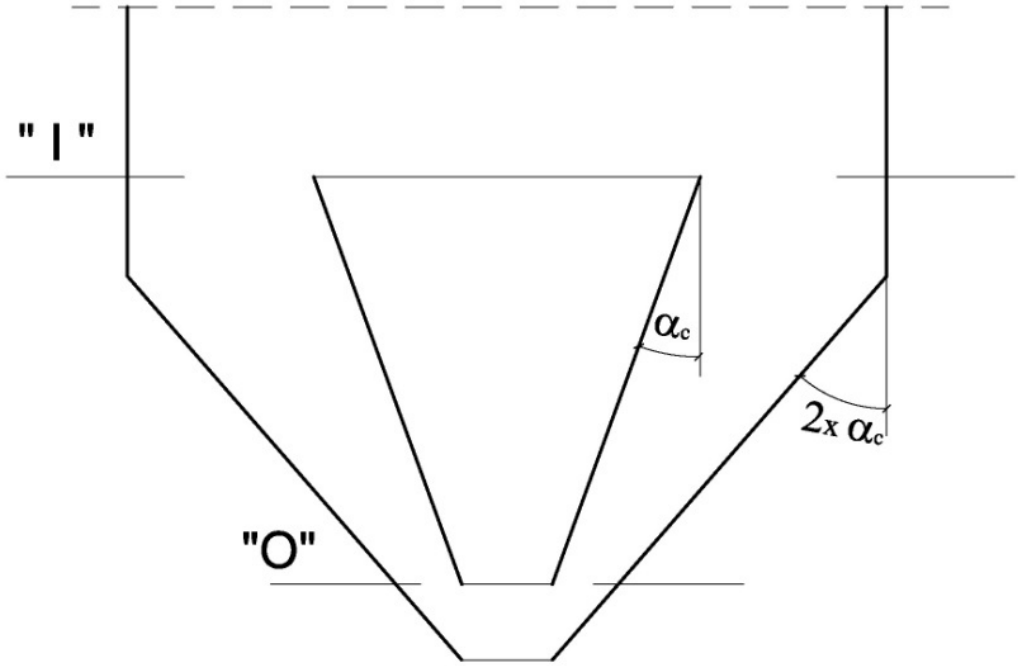

FIGURE 1

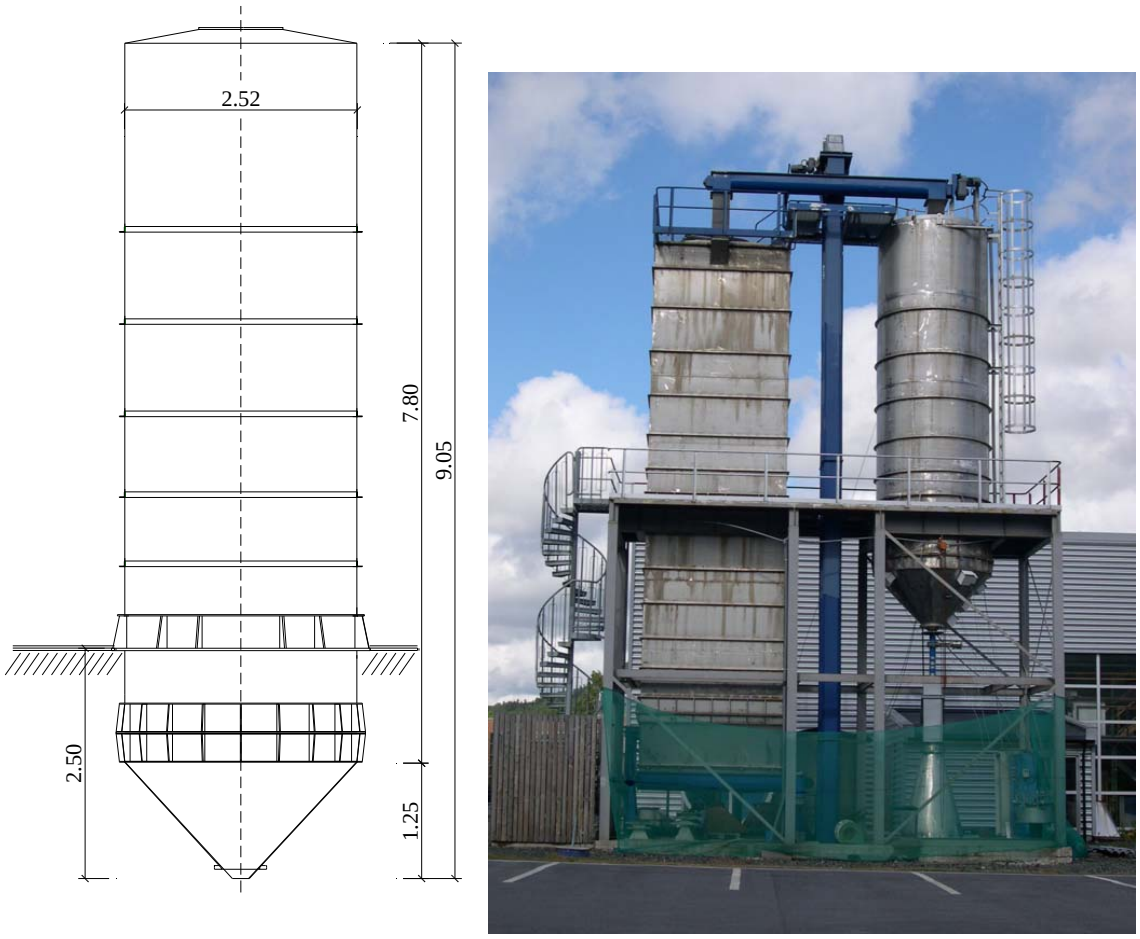

a) b)

FIGURE 2

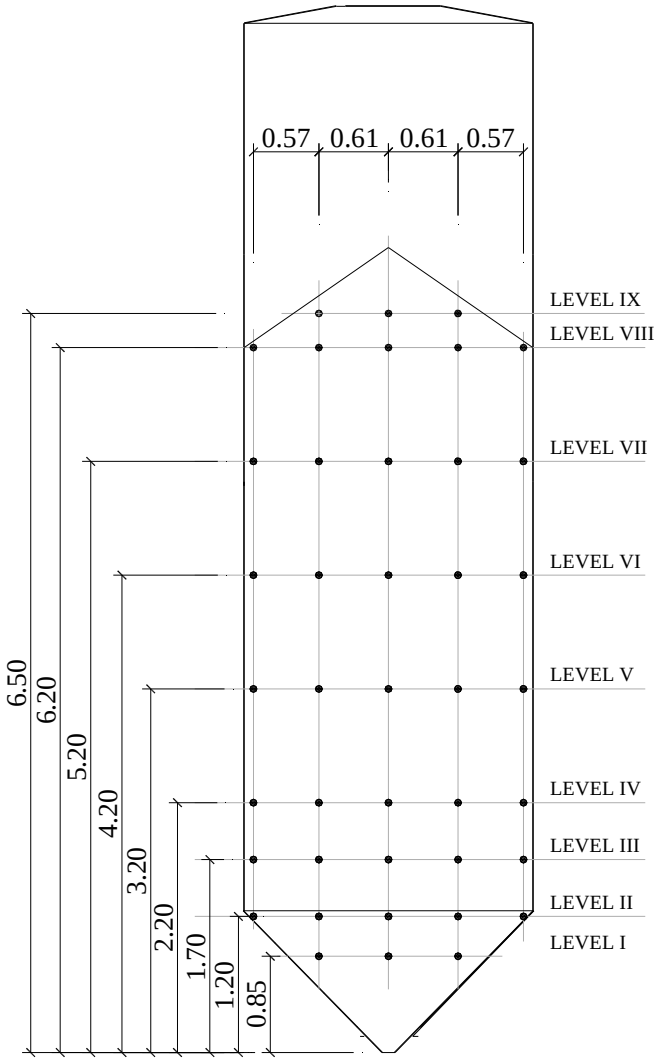
0.57
0.61
0.61
0.57
LEVEL IX
LEVEL VIII
LEVEL VII
LEVEL VI
LEVEL V
LEVEL IV
LEVEL III
LEVEL II
LEVEL I
6.50
6.20
5.20
4.20
3.20
2.20
1.70
1.20
0.85

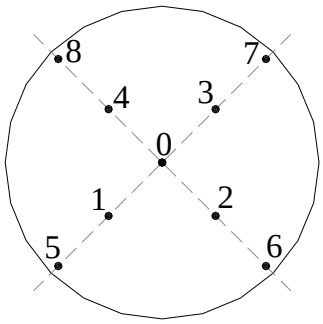
8
7
4
3
0
1
2
5
6

FIGURE 3

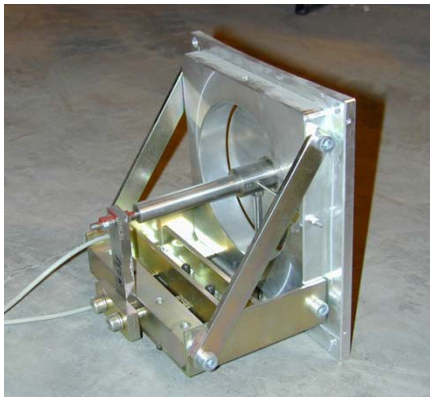

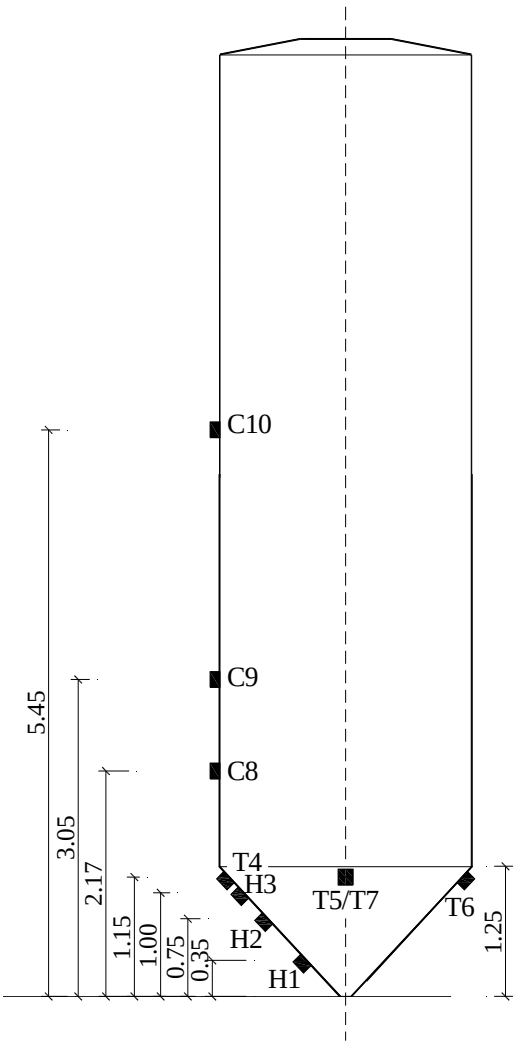

FIGURE 4

a)

b)

c)

FIGURE 5

Silo without inserts - 0
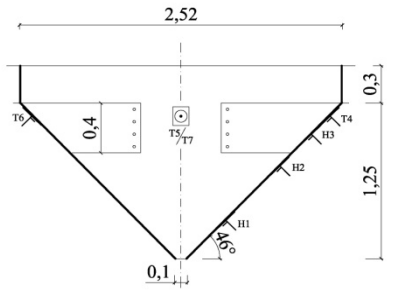

Inverted double cone DC I	Inverted double cone DC II	Double cone DC III
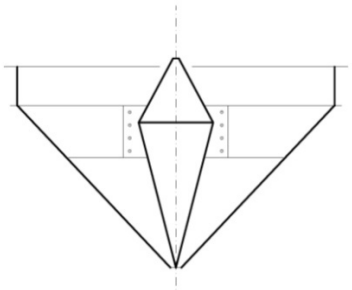	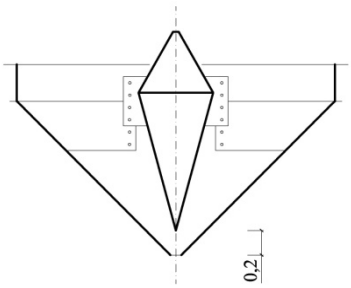	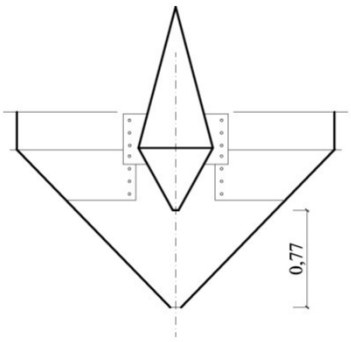

Double cone – DC IV	Skew double cone – DC IVa (non-symmetric position)	Double cone DC V
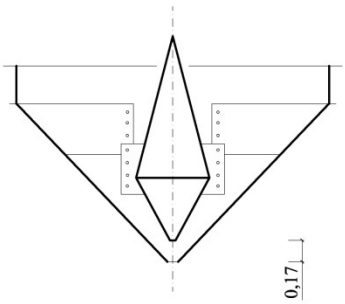	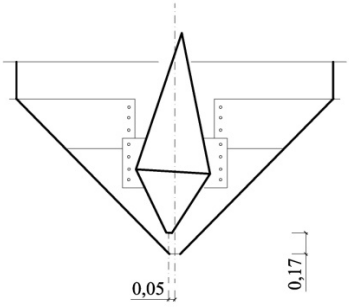	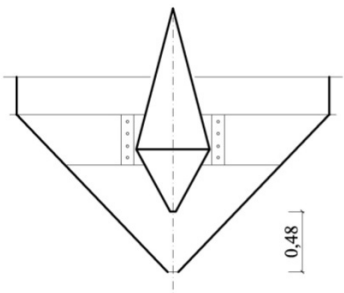

Cone-in-cone CC I	Cone-in-cone CC II	Cone-in-cone CC III
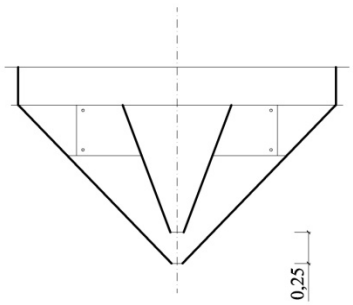	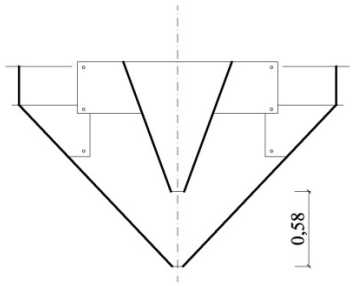	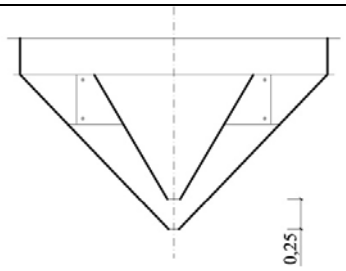

Double cone-in-cone CC IV	Double cone-in-cone CC V	Double cone-in-cone CC VI
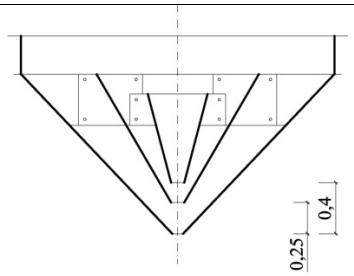	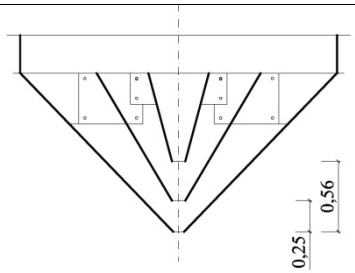	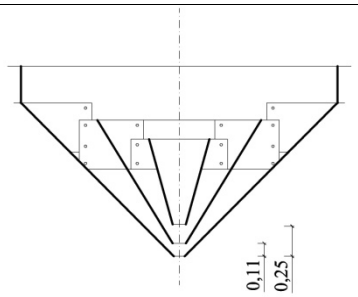

Inverted cone IC I
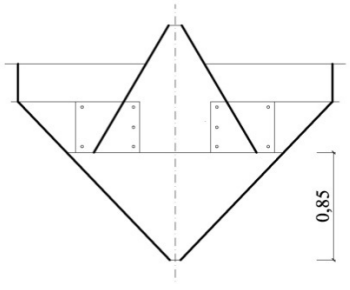

FIGURE 6

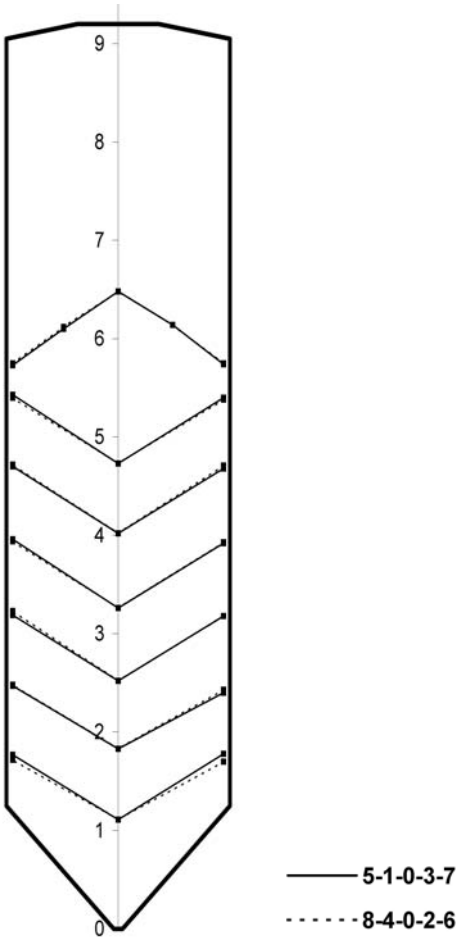
9
8
7
6
5
4
3
2
1
0
5-1-0-3-7
8-4-0-2-6

a)

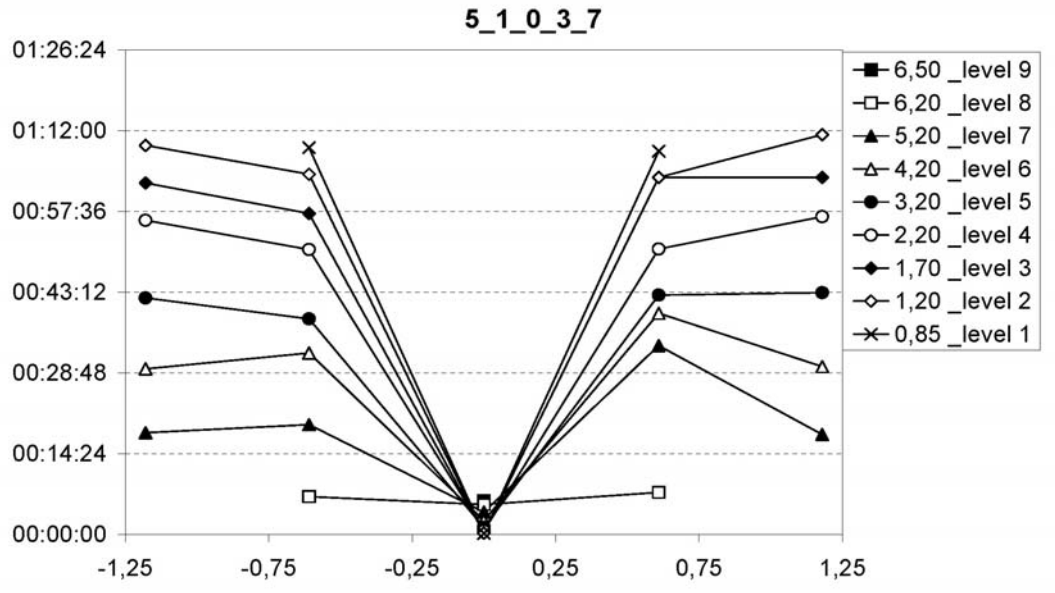
5_1_0_3_7
01:26:24
01:12:00
00:57:36
00:43:12
00:28:48
00:14:24
00:00:00
-1,25
-0,75
-0,25
0,25
0,75
1,25
6,50 _level 9
6,20 _level 8
5,20 _level 7
4,20 _level 6
3,20 _level 5
2,20 _level 4
1,70 _level 3
1,20 _level 2
0,85 _level 1

b)

FIGURE 7

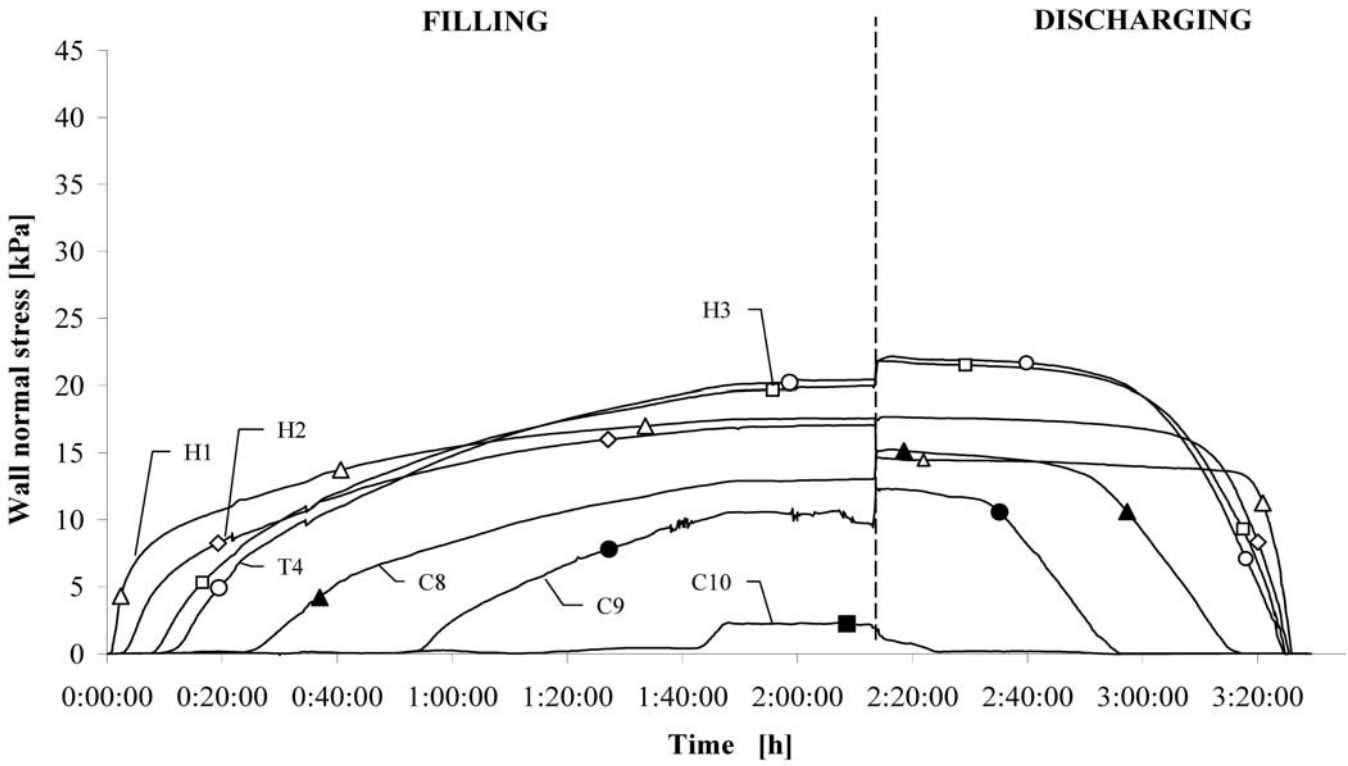
FILLING
DISCHARGING
Wall normal stress [kPa]
45
40
35
30
25
20
15
10
5
0
H1
H2
H3
T4
C8
C9
C10
0:00:00
0:20:00
0:40:00
1:00:00
1:20:00
1:40:00
2:00:00
2:20:00
2:40:00
3:00:00
3:20:00
Time [h]

FIGURE 8

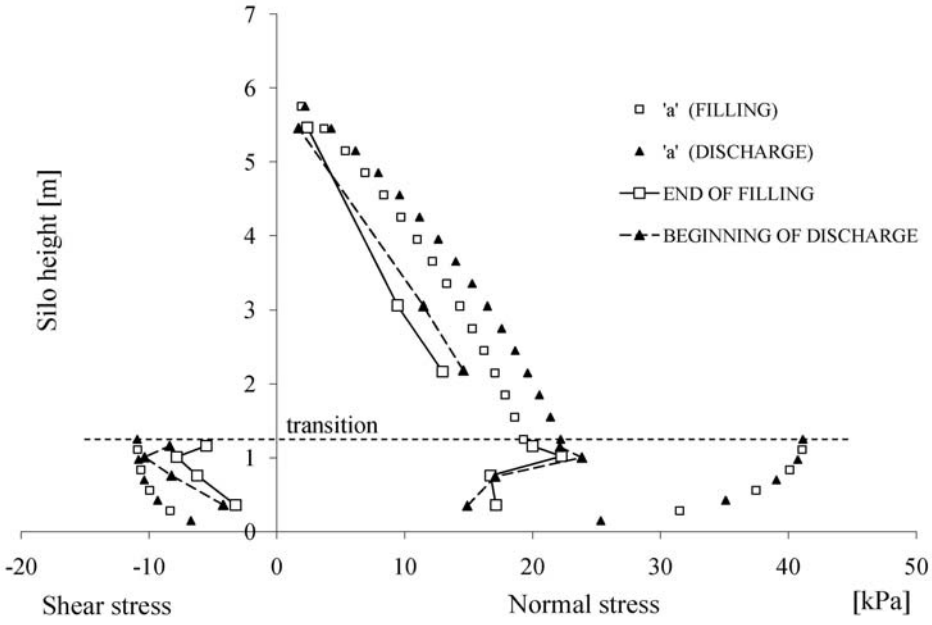
Silo height [m]
7
6
5
4
3
2
1
0
transition
'a' (FILLING)
'a' (DISCHARGE)
END OF FILLING
BEGINNING OF DISCHARGE
-20
-10
0
10
20
30
40
50
Shear stress
Normal stress
[kPa]

a)

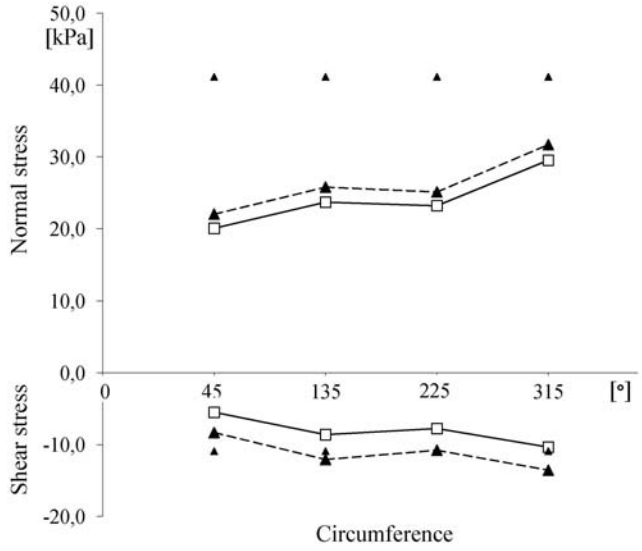
50,0
[kPa]
40,0
30,0
20,0
10,0
0,0
-10,0
-20,0
Normal stress
Shear stress
0
45
135
225
315
[°]
Circumference

b)

FIGURE 9

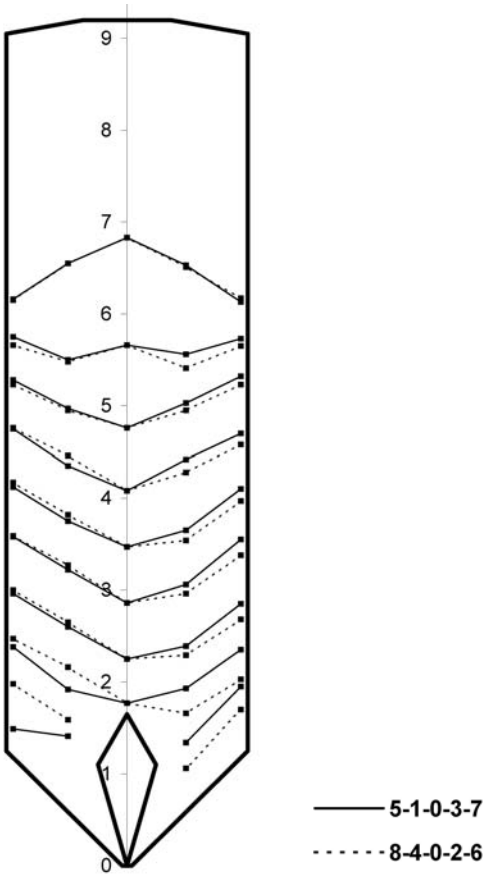
9
8
7
6
5
4
3
2
1
0
5-1-0-3-7
8-4-0-2-6

a)

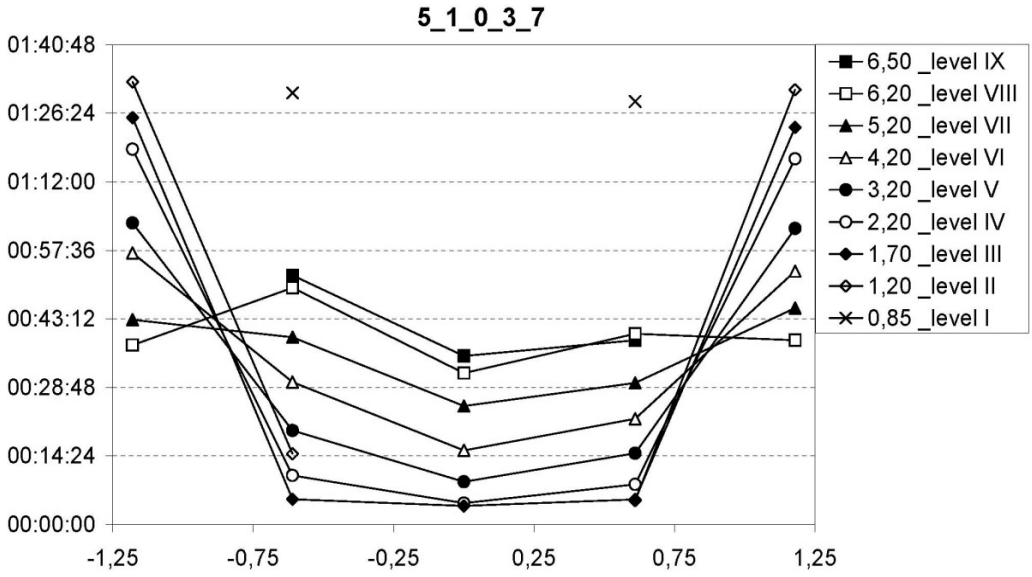
5_1_0_3_7
01:40:48
01:26:24
01:12:00
00:57:36
00:43:12
00:28:48
00:14:24
00:00:00
-1,25
-0,75
-0,25
0,25
0,75
1,25
6,50 _level IX
6,20 _level VIII
5,20 _level VII
4,20 _level VI
3,20 _level V
2,20 _level IV
1,70 _level III
1,20 _level II
0,85 _level I

b)

FIGURE 10

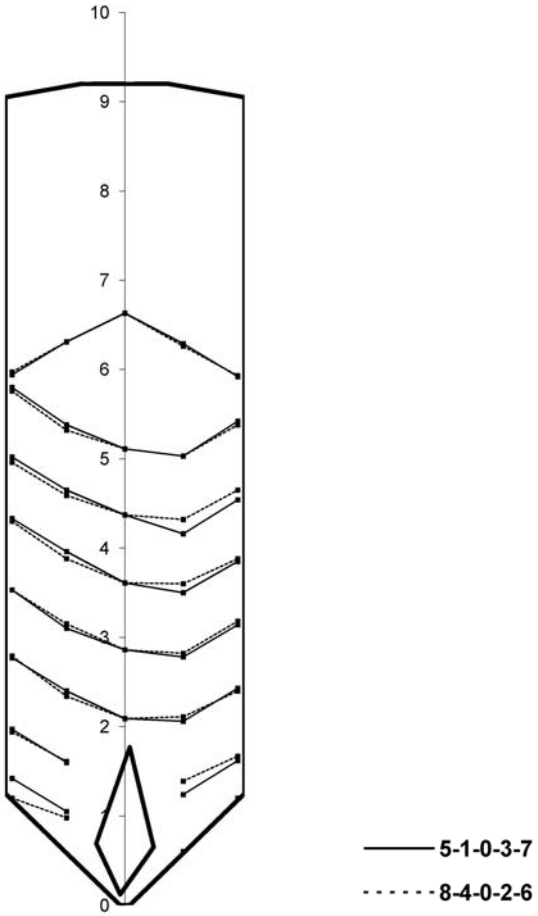
10
9
8
7
6
5
4
3
2
1
0
5-1-0-3-7
8-4-0-2-6

a)

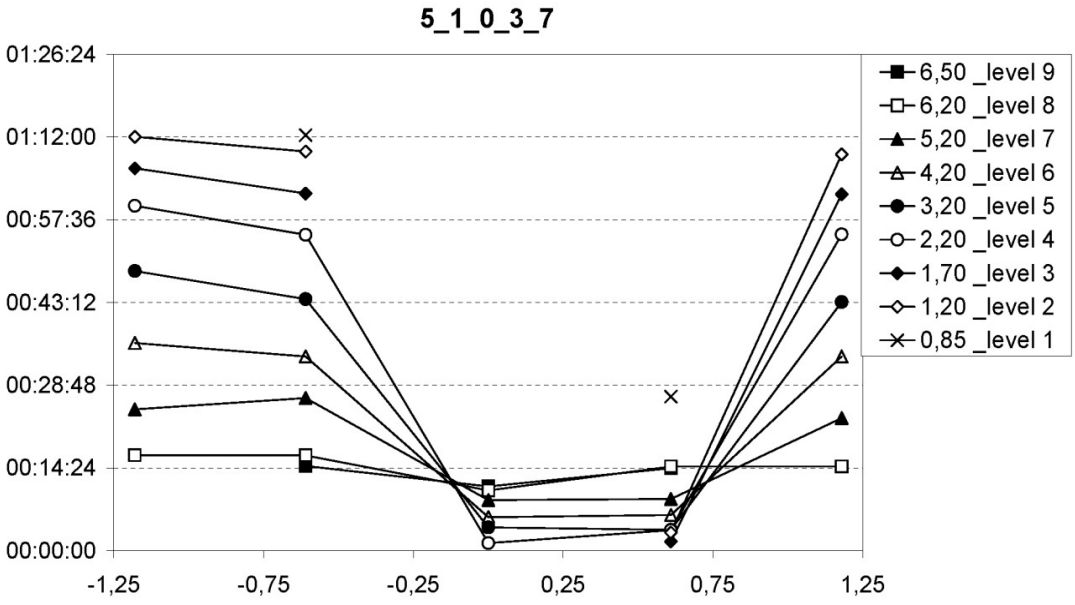
5_1_0_3_7
01:26:24
01:12:00
00:57:36
00:43:12
00:28:48
00:14:24
00:00:00
-1,25
-0,75
-0,25
0,25
0,75
1,25
6,50 _level 9
6,20 _level 8
5,20 _level 7
4,20 _level 6
3,20 _level 5
2,20 _level 4
1,70 _level 3
1,20 _level 2
0,85 _level 1

b)

FIGURE 11

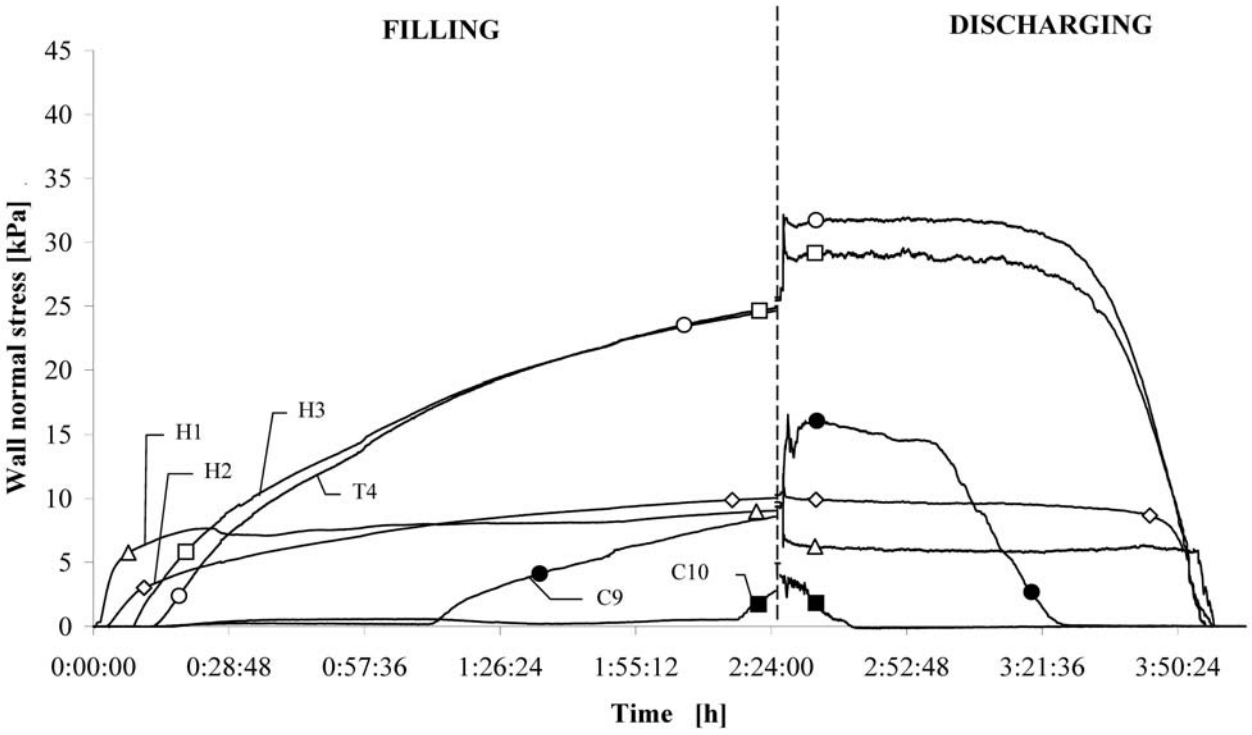
FILLING
DISCHARGING
Wall normal stress [kPa]
45
40
35
30
25
20
15
10
5
0
H1
H2
H3
T4
C9
C10
0:00:00
0:28:48
0:57:36
1:26:24
1:55:12
2:24:00
2:52:48
3:21:36
3:50:24
Time [h]

FIGURE 12

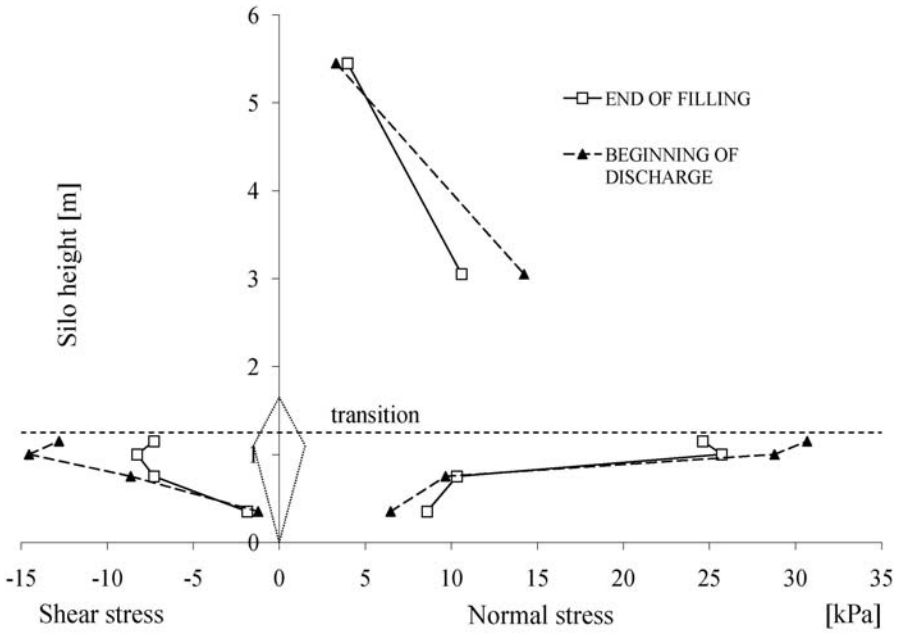
END OF FILLING
BEGINNING OF DISCHARGE
Silo height [m]
transition
Shear stress
Normal stress
[kPa]

a)

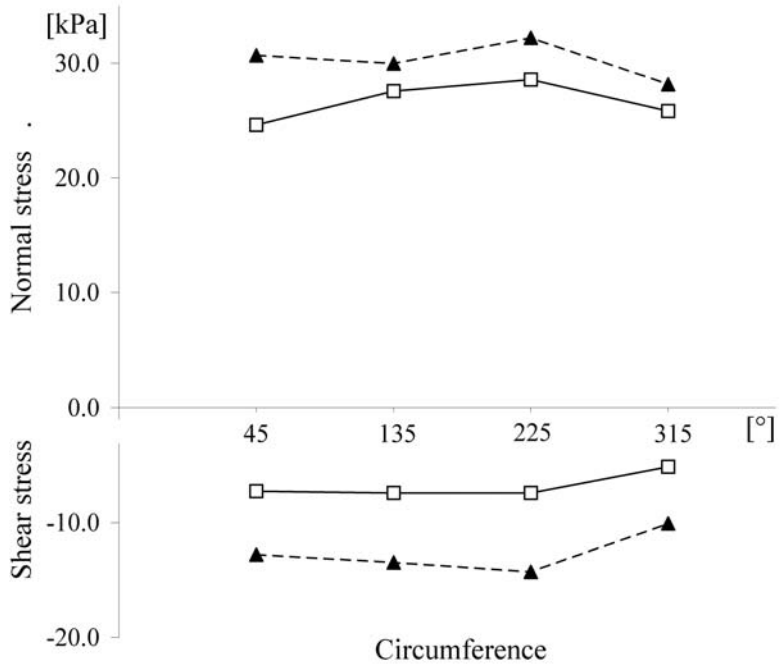
[kPa]
Normal stress
Shear stress
[°]
Circumference

b)

FIGURE 13

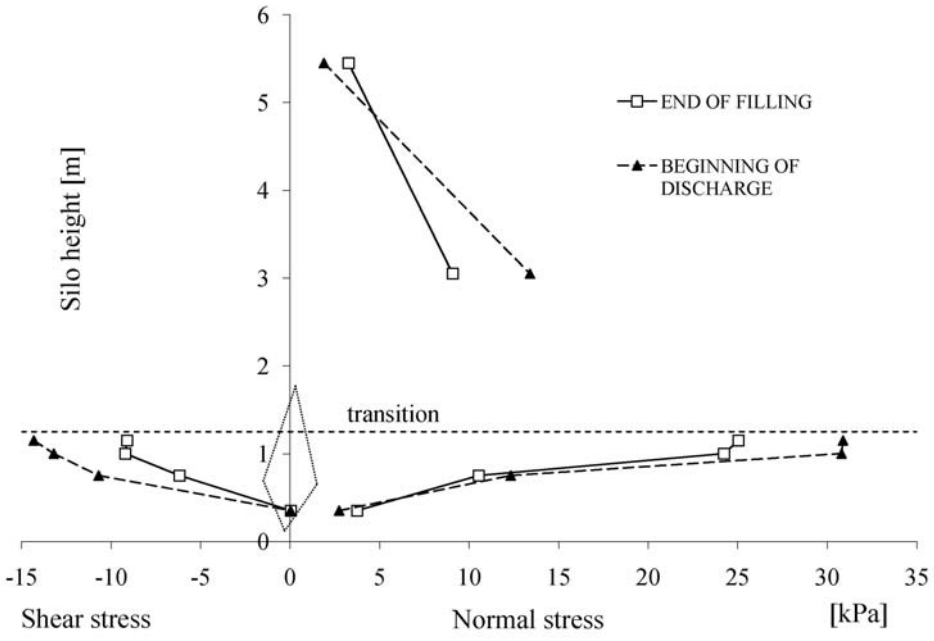
Silo height [m]
END OF FILLING
BEGINNING OF DISCHARGE
transition
Shear stress
Normal stress
[kPa]

a)

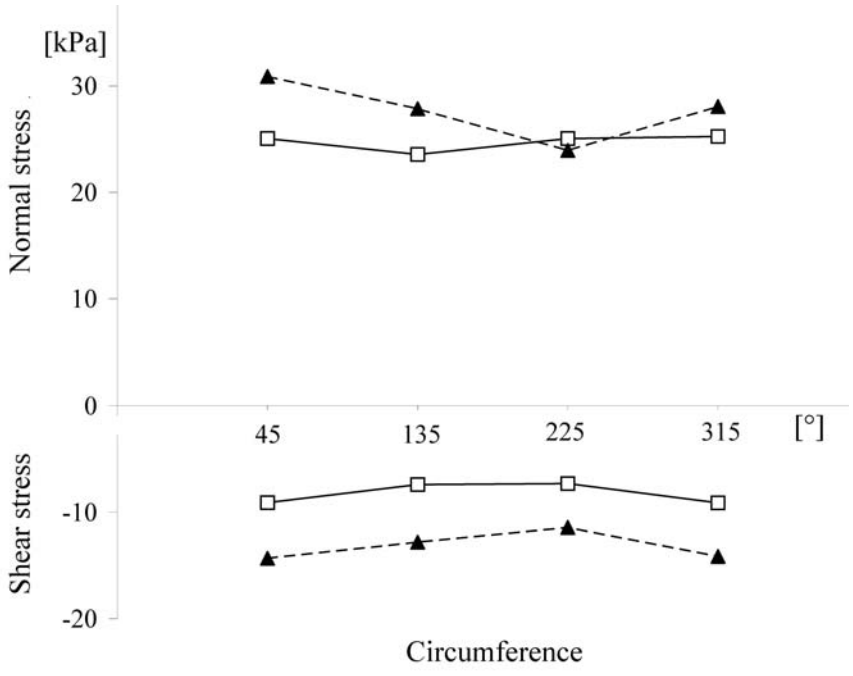
[kPa]
Normal stress
Shear stress
[°]
Circumference

b)

FIGURE 14

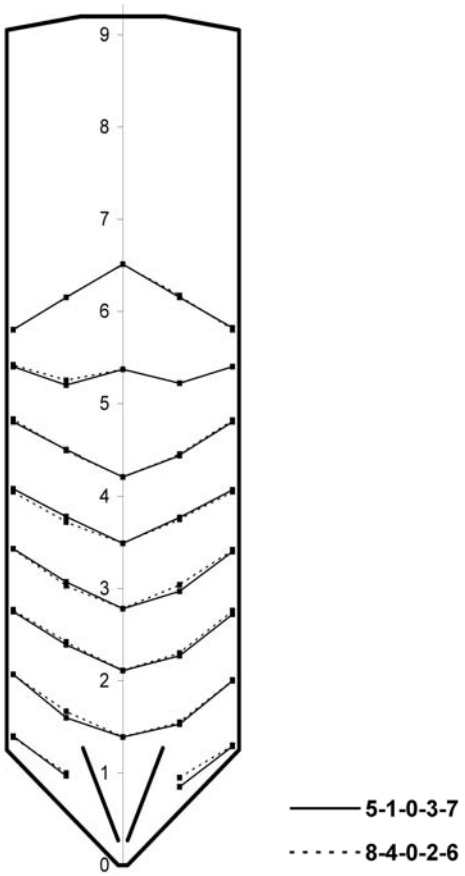
9
8
7
6
5
4
3
2
1
0
5-1-0-3-7
8-4-0-2-6

a)

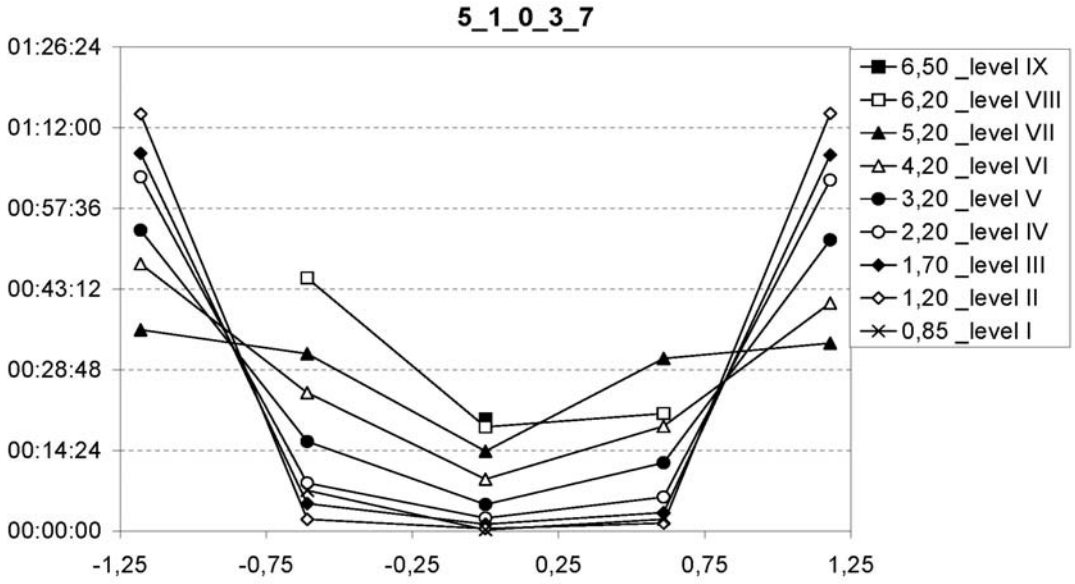
5_1_0_3_7
01:26:24
01:12:00
00:57:36
00:43:12
00:28:48
00:14:24
00:00:00
-1,25
-0,75
-0,25
0,25
0,75
1,25
6,50 _level IX
6,20 _level VIII
5,20 _level VII
4,20 _level VI
3,20 _level V
2,20 _level IV
1,70 _level III
1,20 _level II
0,85 _level I

b)

FIGURE 15

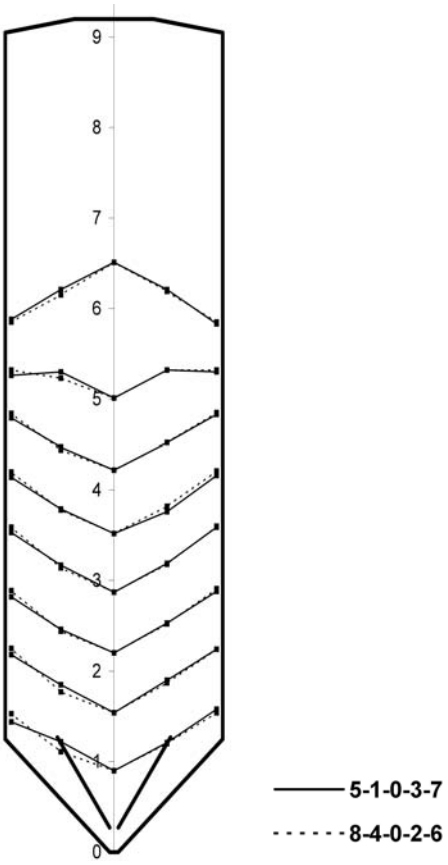
9
8
7
6
5
4
3
2
1
0
5-1-0-3-7
8-4-0-2-6

a)

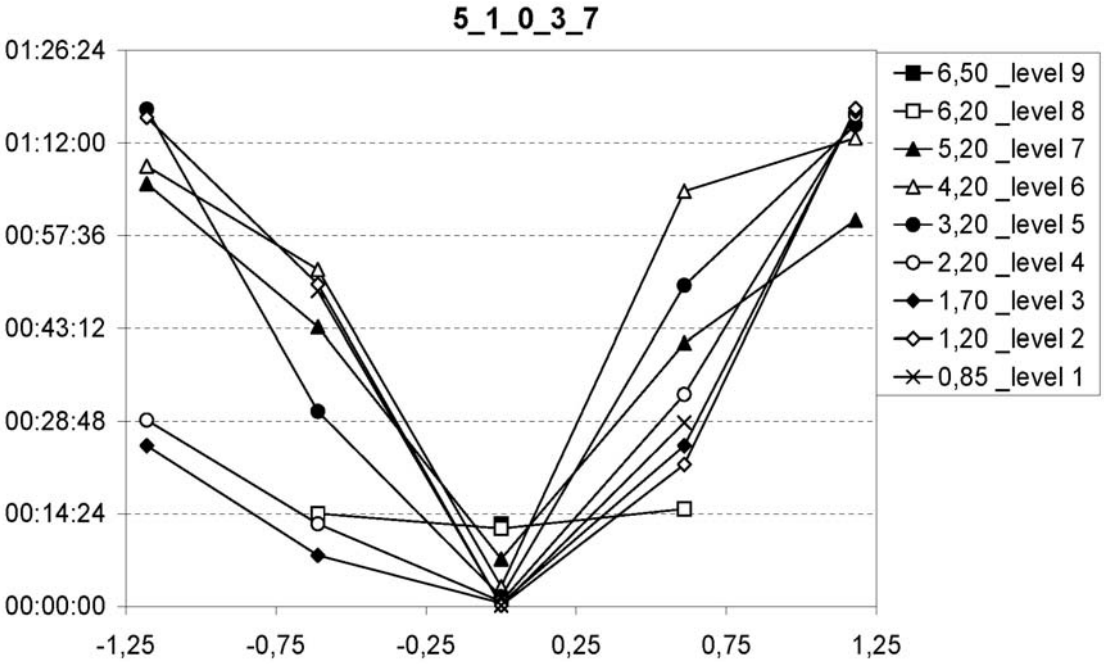
5_1_0_3_7
01:26:24
01:12:00
00:57:36
00:43:12
00:28:48
00:14:24
00:00:00
-1,25
-0,75
-0,25
0,25
0,75
1,25
6,50 _level 9
6,20 _level 8
5,20 _level 7
4,20 _level 6
3,20 _level 5
2,20 _level 4
1,70 _level 3
1,20 _level 2
0,85 _level 1

b)

FIGURE 16

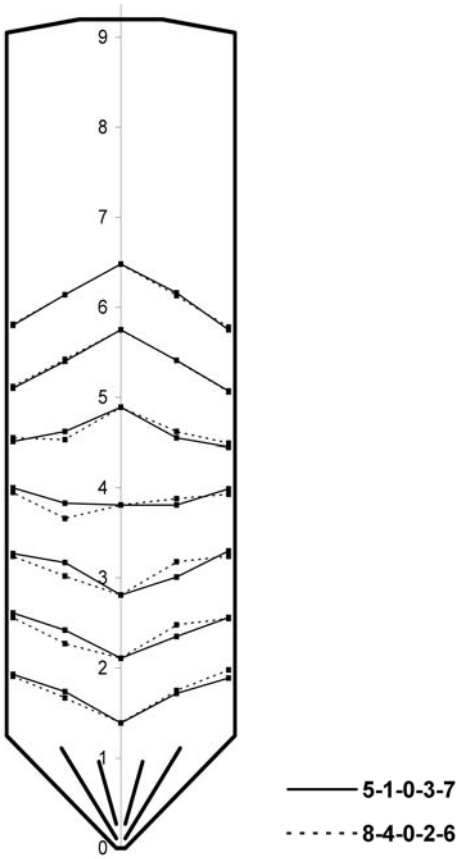
9
8
7
6
5
4
3
2
1
0
5-1-0-3-7
8-4-0-2-6

a)

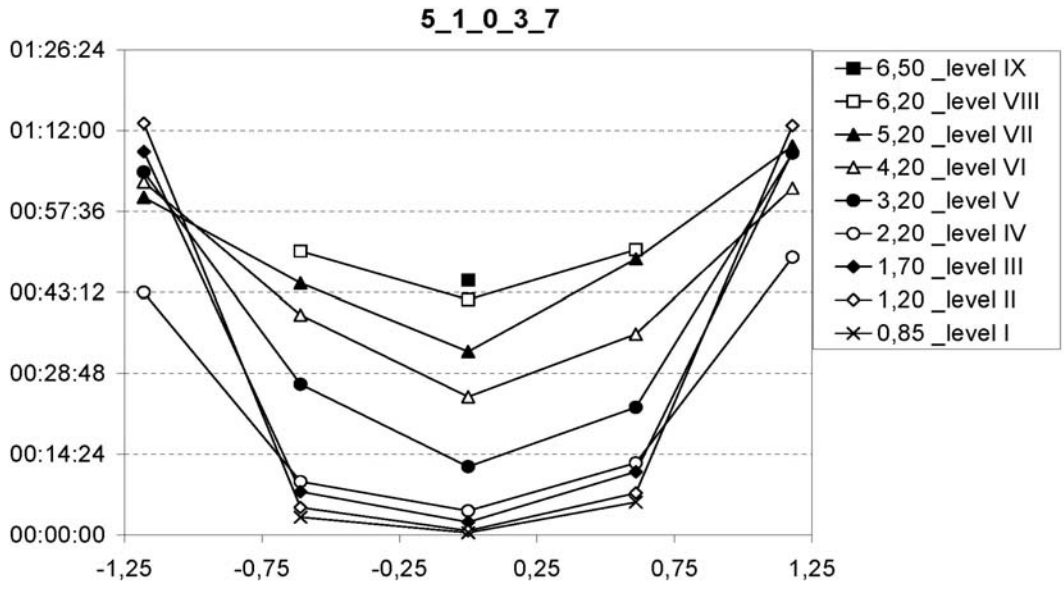
5_1_0_3_7
01:26:24
01:12:00
00:57:36
00:43:12
00:28:48
00:14:24
00:00:00
-1,25
-0,75
-0,25
0,25
0,75
1,25
6,50 _level IX
6,20 _level VIII
5,20 _level VII
4,20 _level VI
3,20 _level V
2,20 _level IV
1,70 _level III
1,20 _level II
0,85 _level I

b)

FIGURE 17

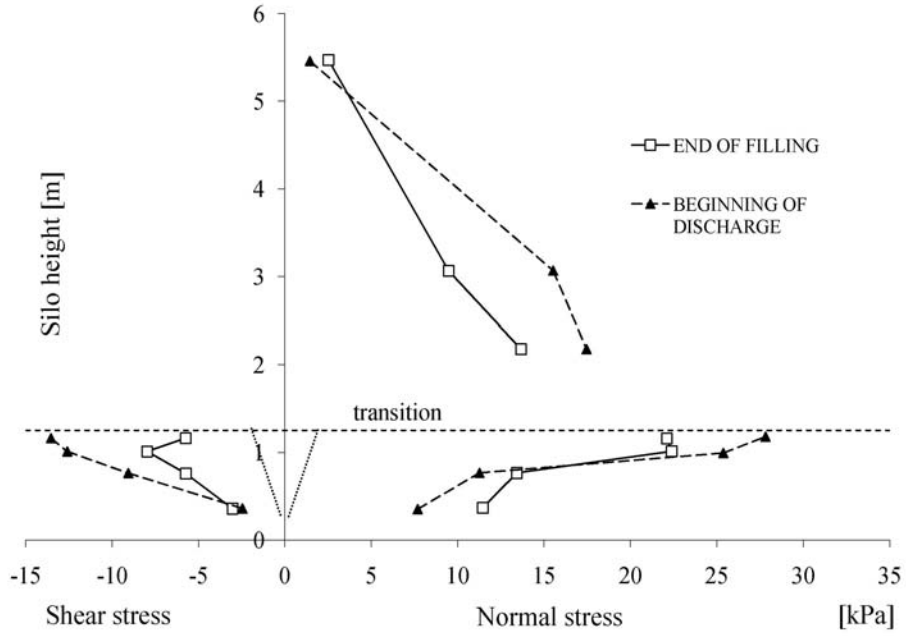
Silo height [m]
END OF FILLING
BEGINNING OF DISCHARGE
transition
Shear stress
Normal stress
[kPa]

a)

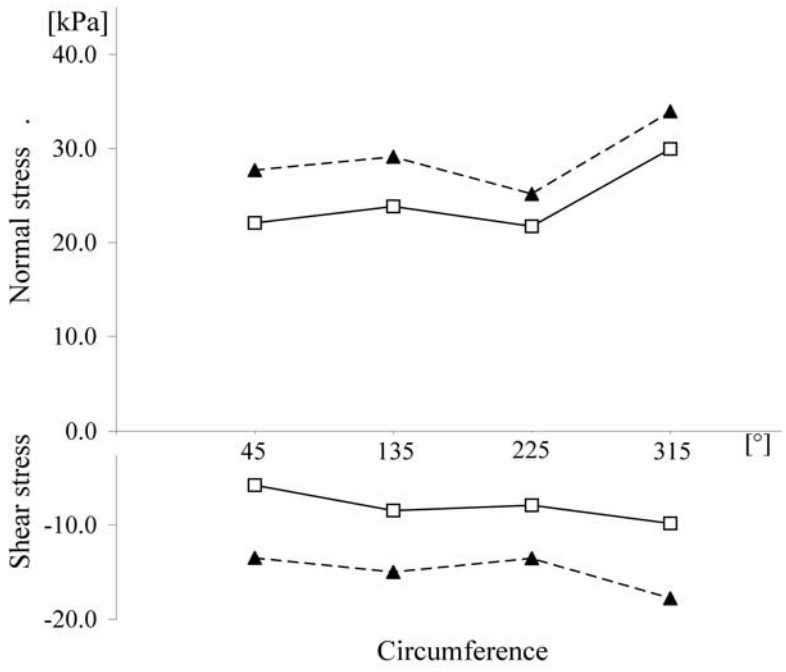
[kPa]
Normal stress
Shear stress
[°]
Circumference

b)

FIGURE 18

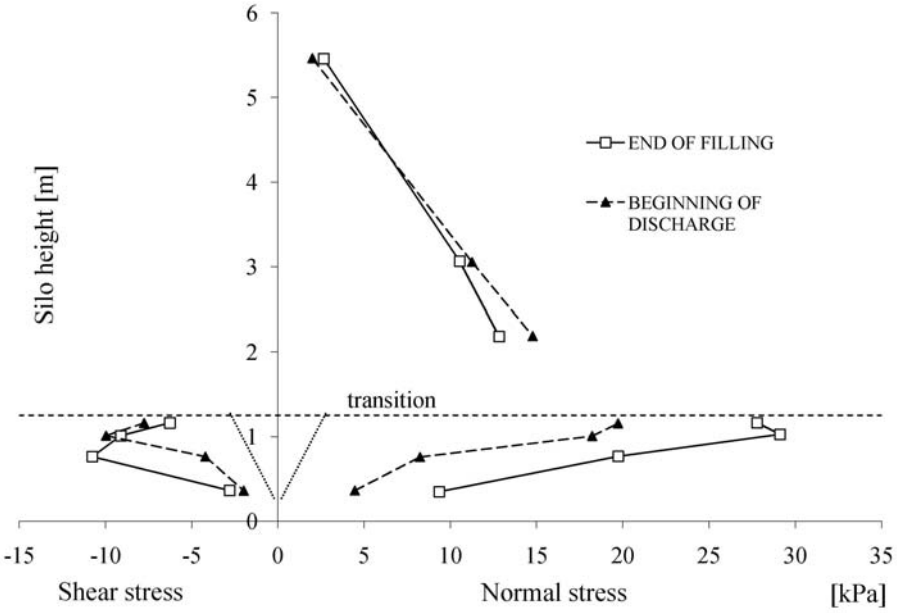
Silo height [m]
END OF FILLING
BEGINNING OF DISCHARGE
transition
Shear stress
Normal stress
[kPa]

a)

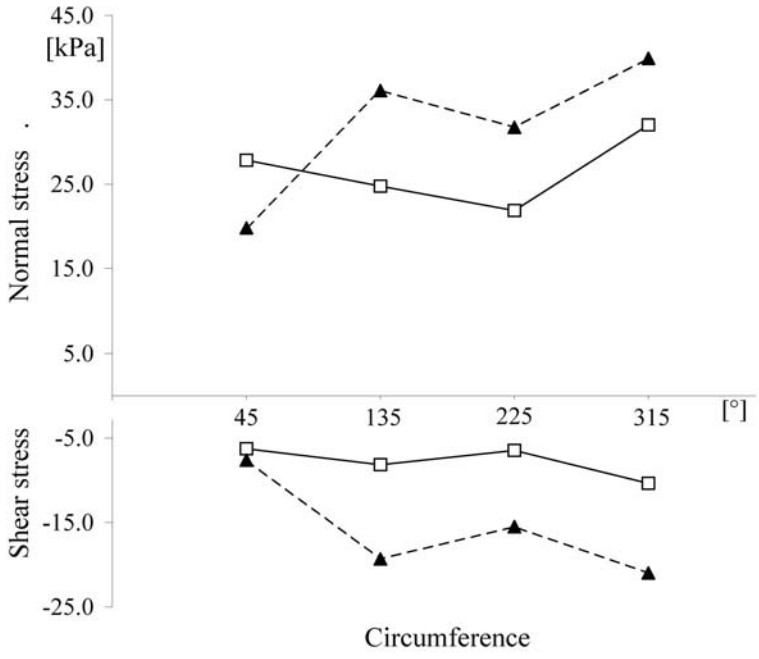
Normal stress
[kPa]
Shear stress
[°]
Circumference

b)

FIGURE 19

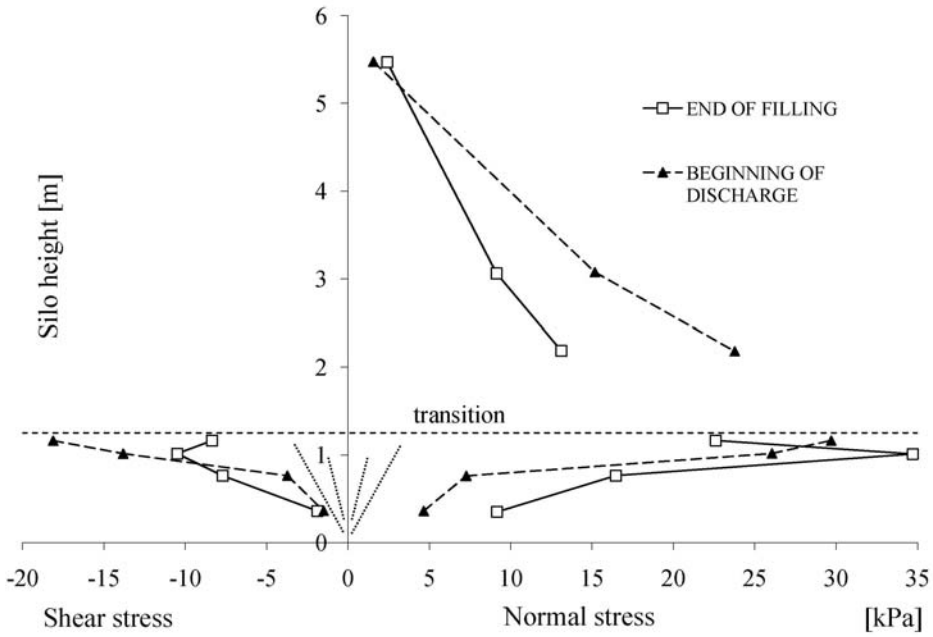
Silo height [m]
6
5
4
3
2
1
0
END OF FILLING
BEGINNING OF DISCHARGE
transition
-20 -15 -10 -5 0 5 10 15 20 25 30 35
Shear stress
Normal stress
[kPa]

a)

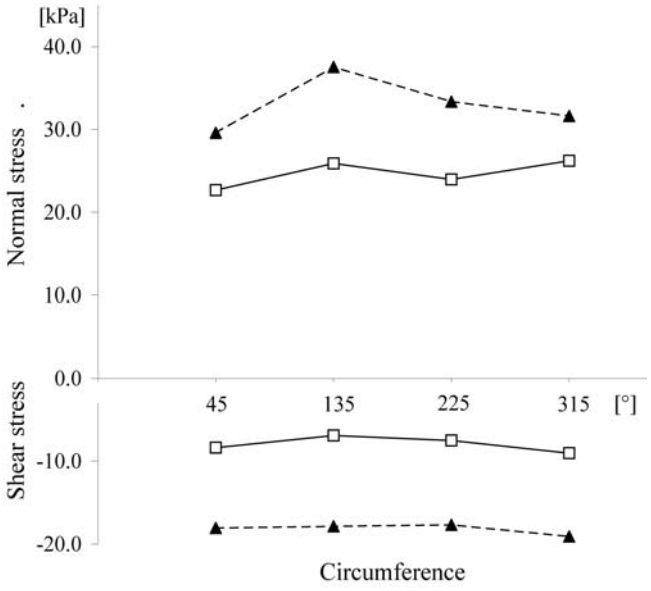
[kPa]
40.0
30.0
20.0
10.0
0.0
Normal stress
45 135 225 315 [°]
Shear stress
-10.0
-20.0
Circumference

b)

FIGURE 20

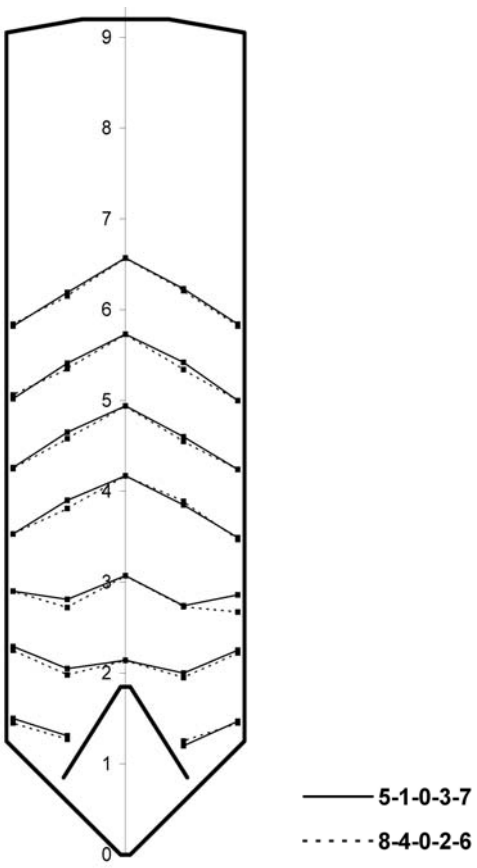
9
8
7
6
5
4
3
2
1
0
5-1-0-3-7
8-4-0-2-6

a)

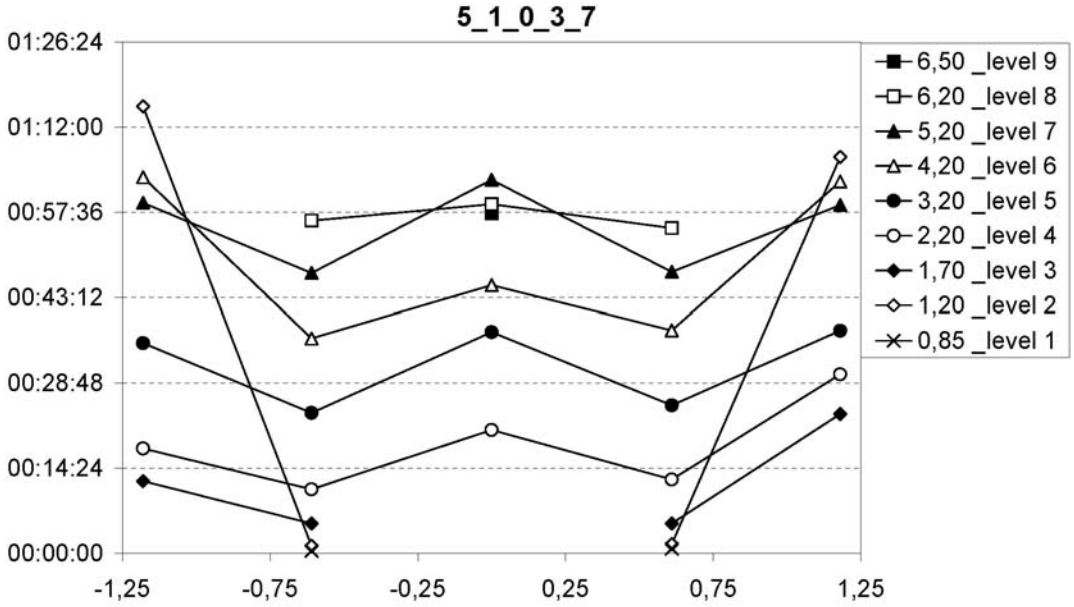
5_1_0_3_7
01:26:24
01:12:00
00:57:36
00:43:12
00:28:48
00:14:24
00:00:00
-1,25
-0,75
-0,25
0,25
0,75
1,25
6,50 _level 9
6,20 _level 8
5,20 _level 7
4,20 _level 6
3,20 _level 5
2,20 _level 4
1,70 _level 3
1,20 _level 2
0,85 _level 1

b)

FIGURE 21

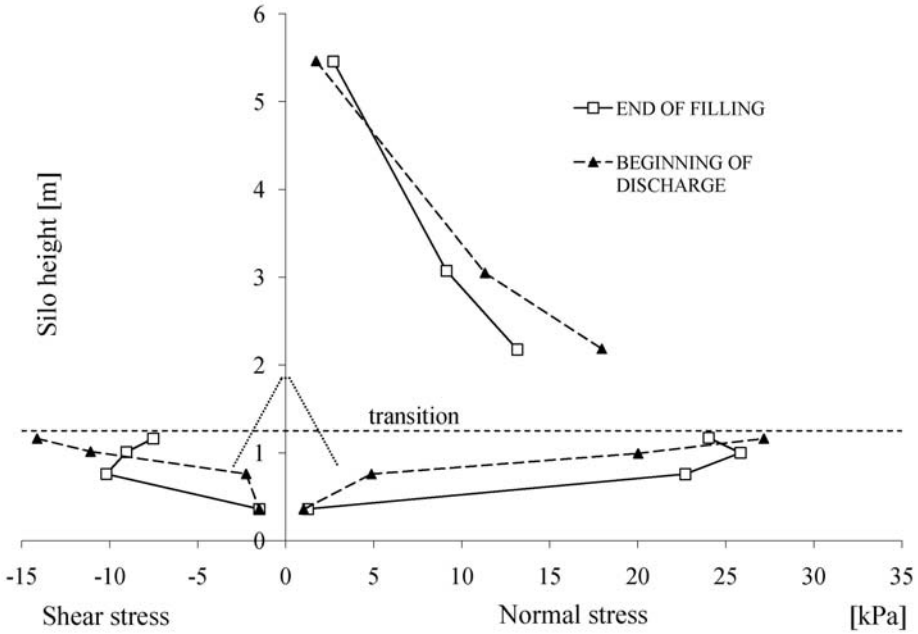
Silo height [m]
END OF FILLING
BEGINNING OF DISCHARGE
transition
Shear stress
Normal stress
[kPa]

a)

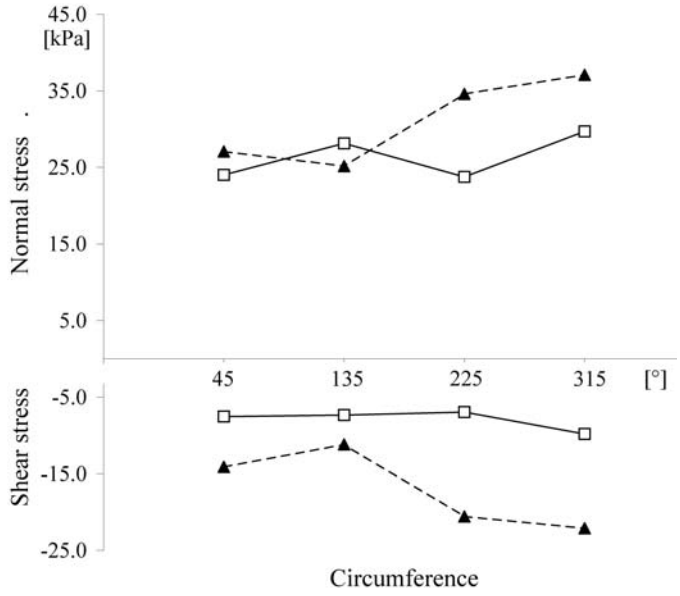
Normal stress
[kPa]
Shear stress
[°]
Circumference

b)

FIGURE 22

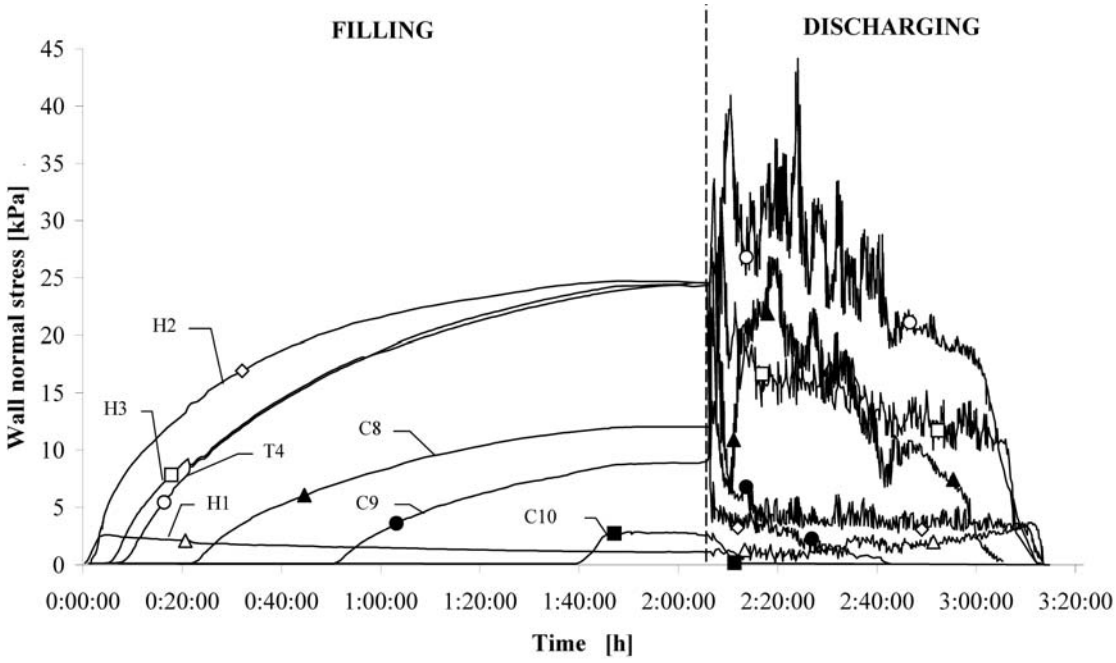
FILLING
DISCHARGING
Wall normal stress [kPa]
45
40
35
30
25
20
15
10
5
0
H2
H3
T4
H1
C8
C9
C10
0:00:00
0:20:00
0:40:00
1:00:00
1:20:00
1:40:00
2:00:00
2:20:00
2:40:00
3:00:00
3:20:00
Time [h]

FIGURE 23

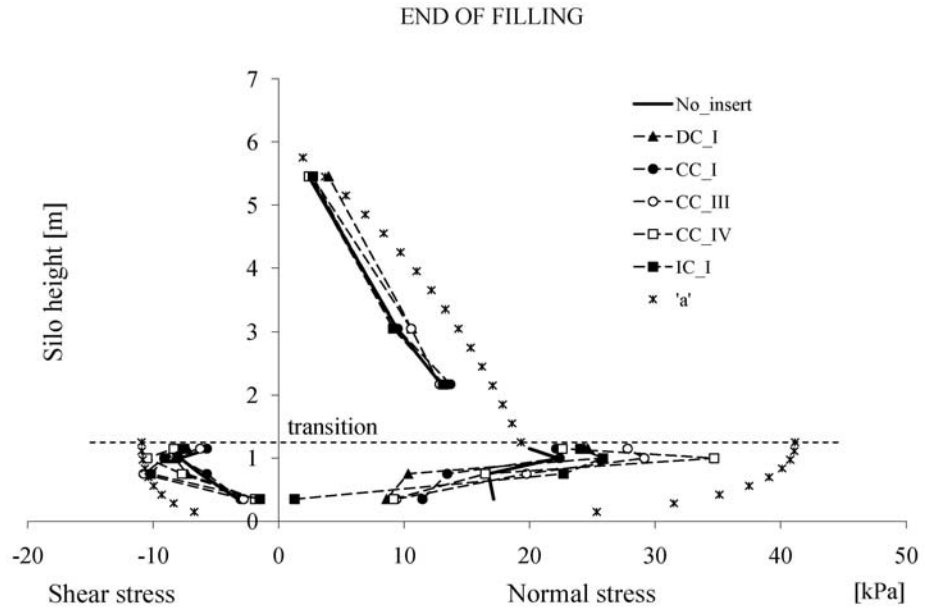
END OF FILLING
Silo height [m]
transition
No_insert
DC_I
CC_I
CC_III
CC_IV
IC_I
'a'
Shear stress
Normal stress
[kPa]

a)

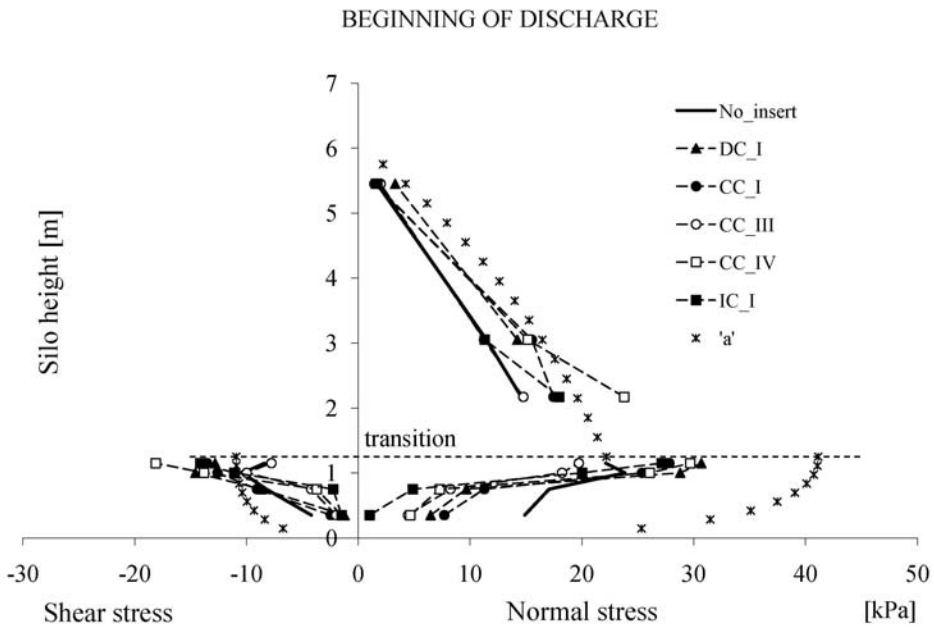
BEGINNING OF DISCHARGE
Silo height [m]
transition
No_insert
DC_I
CC_I
CC_III
CC_IV
IC_I
'a'
Shear stress
Normal stress
[kPa]

b)

FIGURE 24

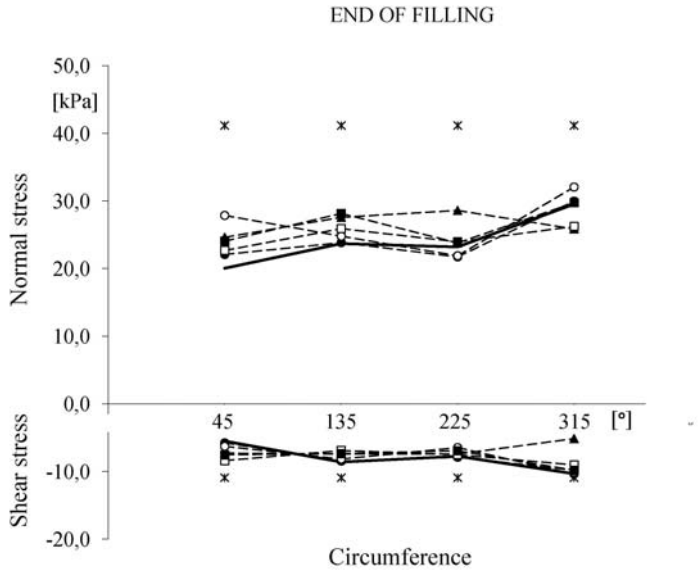
END OF FILLING
50,0
[kPa]
40,0
30,0
20,0
10,0
0,0
-10,0
-20,0
Normal stress
Shear stress
45
135
225
315
[°]
Circumference

a)

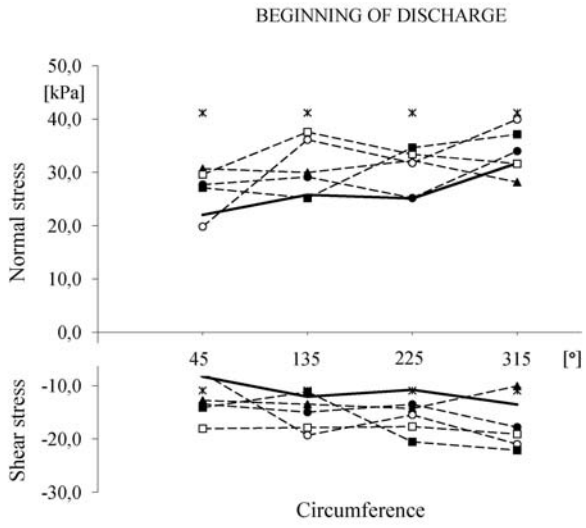
BEGINNING OF DISCHARGE
50,0
[kPa]
40,0
30,0
20,0
10,0
0,0
-10,0
-20,0
-30,0
Normal stress
Shear stress
45
135
225
315
[°]
Circumference

b)

FIGURE 25